



## Research paper

## Structural isomers of cinnamic hydroxamic acids block HCV replication via different mechanisms

Maxim V. Kozlov\*, Konstantin A. Konduktorov, Alsu Z. Malikova<sup>1</sup>, Kamila A. Kamarova, Anastasia S. Shcherbakova, Pavel N. Sol'yev, Sergey N. Kochetkov

Engelhardt Institute of Molecular Biology, Russian Academy of Sciences, Vavilova 32, Moscow, 119991, Russia

## ARTICLE INFO

## Article history:

Received 25 August 2019

Accepted 19 September 2019

Available online xxx

## Keywords:

Cinnamic hydroxamic acids

Anti-HCV activity

Cell viability

Inhibition of histone deacetylases

## ABSTRACT

A set of *ortho*-, *meta*- and *para*-substituted cinnamic hydroxamic acids (CHAs) was synthesized. In each series of structural isomers, a phenyl substituent was linked to an aromatic ring of the parent cinnamic acid via a linker of one to four atoms in length. Using a cell test system with the full-length replicon of hepatitis C virus (HCV), we established a relationship between the suppression of HCV replicon propagation and the inhibition of class I/IIb histone deacetylases (HDACs). Anti-HCV activity correlated with the inhibition of HDAC8 in the case of *ortho*-CHAs, while in the case of *meta*-CHAs it correlated with the inhibition of HDAC1/2/3 and HDAC6. The antiviral activity of *para*-CHAs was many times stronger than that of *meta*-CHAs with about the same efficiency of HDAC1/2/3/6 inhibition, which indicated the existence of an additional cell target that does not belong to the studied group of HDACs.

© 2019 Elsevier Masson SAS. All rights reserved.

## 1. Introduction

The success achieved in the therapy of chronic hepatitis C (CHC) due to the creation of effective direct acting antivirals (DAAs) provides an opportunity to search for new approaches to the treatment of CHC, including the development of antiviral host targeting agents (HTAs) [1]. The combined application of DAAs and HTAs appears promising – hypothetically, it can lead to a sustained virologic response with a short duration of the therapy, thereby reducing the risk of emergence of DAA-resistant strains of hepatitis C virus (HCV) [2].

Histone deacetylases (HDACs) are of interest as anti-HCV host targets due to a close interweaving of HCV propagation and activities of HDACs. Very recently, Hamdane et al. have convincingly demonstrated a major epigenetic reprogramming in the hepatocytes of patients with CHC, which correlates with specific genome-wide changes in the acetylated form of histone H3 (H3K27ac) [3]. Earlier, Chen et al. have shown that both gluconeogenic activity and HDAC9 expression levels are increased in liver tissues from HCV-infected patients, and the key role in abnormal glucose homeostasis is played by HDAC3/9-dependent deacetylation of the

transcription factor FoxO1 [4,5].

HDACs form an extensive family of enzymes which includes zinc-dependent HDACs classes I, II, and IV that hydrolyze the  $\epsilon$ -N-acetyllysine residues of protein substrates, coordinating the oxygen atom of the acetyl group with zinc ion. HDACs class III, also referred to as SIRT6 (sirtuins), use the coenzyme NAD<sup>+</sup> for deacetylation [6]. As for zinc-dependent HDACs, they can be located either in the nucleus (HDAC1/2/3 class I), or in the nucleus and cytoplasm (HDAC8 class I and HDAC4/5/7/9 class IIa), or in the cytoplasm (HDAC6/10 class IIb and HDAC11 class IV). It is likely that HDACs class IIa do not have an independent deacetylation activity, but after entering the nucleus, they interact with HDAC3 comprising a part of regulatory transcription complexes and play the role of signal transducers [7,8].

Epigenetic changes induced by HCV may be caused by the activation of HDACs, which is promoted by oxidative stress [9]. The observed increase in the activity of nuclear HDACs led to a decrease in the level of H3K9ac and suppression of expression of a negative regulator of iron absorption, hepcidin. It is worth noting that the inhibition of HDACs with a small molecule compound, trichostatin A, caused the simultaneous accumulation of H3K9ac, activation of hepcidin expression, and suppression of HCV replication [10]. Subsequent use of the acetyl-histone H3 chromatin immunoprecipitation assay allowed to identify two more genes – osteopontin (OPN) and apolipoprotein-A1 (Apo-A1), the expression of which,

\* Corresponding author.

E-mail address: [kozlovmv@eimb.ru](mailto:kozlovmv@eimb.ru) (M.V. Kozlov).<sup>1</sup> Deceased.

similar to the expression of the hepcidin gene (*LEAP-1*), is closely interconnected with HCV infection and HDAC inhibition [11,12].

HDAC6 has a strong nuclear export signal that results in the cytoplasmic retention of HDAC6, which excludes its participation in histone deacetylation [13]; nonetheless, a selective inhibition of HDAC6 leads to suppression of HCV replication [14]. Deacetylating activity towards numerous proteins, enzymes and transcription factors as well as ubiquitin-binding activity and interaction with a molecular motor, dynein, make HDAC6 involved in the most important cellular processes (cell division, oxidative stress, autophagy etc) that can both contribute to viral infection and counteract it [15–17]. Unfortunately, the inherent polyfunctionality of HDAC6 makes it difficult to identify the mechanisms of its influence on HCV replication.

The activity of both nuclear and cytoplasmic HDACs is suppressed in the presence of a variety of hydroxamic inhibitors, including derivatives of cinnamic hydroxamic acid (CHAs) [18]. In the structure of CHAs, the phenyl residue of cinnamic acid (*linker*) is most often bound to a hydrophobic aromatic or heterocyclic substituent (*cap*) via a *connection unit*, the length of which usually does not exceed four atoms. The introduction of a suitable substituent dramatically increases affinity of HDAC inhibitors due to an additional interaction with the active site of the enzyme. While *para* and *meta* derivatives of CHA are multipotent inhibitors of histone deacetylases, *ortho* derivatives often exhibit selectivity for HDAC8 [19].

The SAR studies of CHAs as inhibitors of HCV replication demonstrated that the introduction of small substituents (Me, MeO, CF<sub>3</sub>, etc.) into the phenyl ring or exocyclic cinnamic acid residue significantly affected the potency of anti-HCV action of CHAs [20,21]. Predictably, the introduction of more bulky pyridyl-4-oxy-substituent into different positions of the phenyl ring of CHAs not only changed the potency of HCV suppression, but also affected the selectivity of HDAC inhibition [22]. In this work, we synthesized a set of structural *ortho*, *meta* and *para* isomers of phenyl derivatives of CHA with *connection units* of various lengths. Using a test system with the full-length HCV replicon, we evaluated the potency of inhibition of HCV replication in parallel with the acetylation of HDACs protein substrates for each series of compounds. Our data clearly indicate a correlation between the inhibition of HDACs and anti-HCV action of *ortho*- and *meta*-CHAs, while the antiviral activity for *para*-CHAs was most likely determined by a different cell target.

## 2. Results and discussion

### 2.1. Chemistry

A set of 15 compounds was synthesized according to the common synthetic procedures shown in Scheme 1. At the final stage, hydroxamic acids were prepared by means of activation of the corresponding cinnamic acids by carbonyldiimidazole in DMF with subsequent hydroxyaminolysis, as described earlier [21]. At the previous stage, commercially not available cinnamic acids (CAs) were synthesized by the Knoevenagel condensation of corresponding benzaldehydes with malonic acid. And at the first stage of

synthesis, isomeric hydroxybenzaldehydes were alkylated with phenethyl bromide or 2-phenoxyethyl bromide in DMF in the presence of K<sub>2</sub>CO<sub>3</sub> as a base. The length of *connection unit* between the phenyl rings of the substituent and the cinnamic acid residue varied from 1 to 4 atoms; as for *ortho*-, *meta*- and *para*-methoxy derivatives of CHA, they were used in the biological assays as reference compounds that do not possess a *cap* structure.

### 2.2. Antiviral activity and cytotoxicity

All synthesized *ortho*-, *meta*- and *para*-CHAs were tested as antiviral agents in the cell test system with the full-length HCV replicon that additionally encodes the luciferase gene. The strength of the chemiluminescent signal obtained in the described assay was proportional to the amount of viral RNA [23]. In parallel, the effect on cell viability was determined for all compounds using the MTT test. The results of testing are presented in detail in Table 1 and for greater clarity are reproduced on a three-dimensional histogram (Fig. 1A).

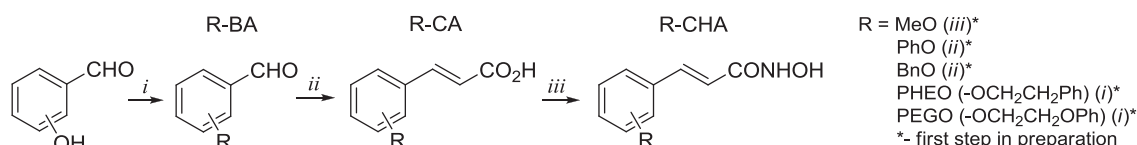
As can be seen from Fig. 1A: (i) *para*-PhO/BnO/PHEO-CHAs blocked HCV replication many times more strongly than *ortho* and *meta* analogues; (ii) *ortho*-PhO/BnO/PHEO/PEGO-CHAs were significantly less cytotoxic than *meta* and *para* analogues; (iii) in comparison with MeO derivatives, phenyl *ortho* and *para*, but not *meta* derivatives of CHA demonstrated an increased selectivity of antiviral action; (iv) differences in the antiviral properties of *meta*- and *para*-, but not *ortho*-PEGO-CHAs, were diminished due to the *connection unit* length of 4 atoms.

Based on the results of testing of the entire set of compounds, a scatter plot (Fig. 1B) of cytotoxicity versus antiviral activity expressed as pCC<sub>50</sub> and pEC<sub>50</sub>, respectively, was constructed; a significant moderate positive correlation was found between them ( $r = 0.520$ ,  $P < 0.05$ ). However, it is easy to see that a selection of five *meta*-CHAs, together with two methoxy *ortho* and *para* derivatives, formed a separate group of compounds ('5 m+2 M'), the antiviral activity of which statistically correlated with cytotoxic effect significantly stronger and more reliably ( $r_m = 0.950$ ,  $P < 0.002$ ). As expected, on the scatter plot of pEC<sub>50</sub> versus lg(TI), an indicator of the selectivity of the antiviral effect, the values of lg(TI) for compounds of the '5 m+2 M' group were minimal and were located in the narrow range of values – 0.31 (Fig. 1C). At the same time, phenyl *ortho* and *para* derivatives of CHA demonstrated the values of lg(TI)  $\geq 2$ , which gives the evidence to suggest that the mechanism of HCV replication suppression is not associated with the cytotoxic effect of these compounds.

### 2.3. Inhibition of HDACs

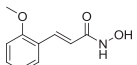
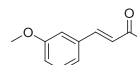
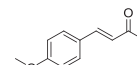
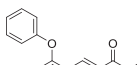
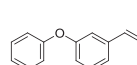
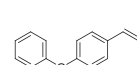
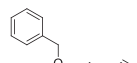
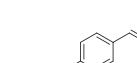
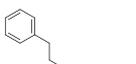
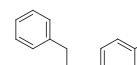
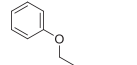
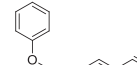
#### 2.3.1. Inhibition of HDAC1/2/3

Our interest in the relationship between suppression of HCV replication by CHAs and their inhibition of HDACs class I was generated by convincing data on the involvement of these enzymes in the development of HCV infection [3,9–12]. However, it is obvious that deregulation of gene expression in the presence of CHAs may also be the cause of the cytotoxic effect of these compounds. An analysis of the scatter plots of inhibition of HDACs class



**Scheme 1.** Reagents and conditions: (i) RBr, K<sub>2</sub>CO<sub>3</sub>, DMF, 70–90 °C, 1–2 h; (ii) HO<sub>2</sub>CCH<sub>2</sub>CO<sub>2</sub>H, (CH<sub>2</sub>)<sub>5</sub>NH, Py, 120 °C, 3 h; (iii) CDI, DMF, 2 h followed by NH<sub>2</sub>OH·HCl overnight.

**Table 1**  
Anti-HCV activity and cytotoxicity of tested CHAs<sup>a</sup>.

R <sup>b</sup> /L <sup>b</sup>	Structure and denotation of R-CHAs EC <sub>50</sub> (μM) <sup>c</sup> /CC <sub>50</sub> (μM) <sup>c</sup> /TI (= CC <sub>50</sub> /EC <sub>50</sub> )		
MetO/1	 <i>ortho</i> -MeO-CHA 1.1 ± 0.17/30 ± 7.5/27	 <i>meta</i> -MeO-CHA 0.57 ± 0.14/17 ± 3.4/30	 <i>para</i> -MeO-CHA 0.56 ± 0.040/15 ± 4.5/27
PhO/1	 <i>ortho</i> -PhO-CHA 0.40 ± 0.10/66 ± 9.4/165	 <i>meta</i> -PhO-CHA 0.40 ± 0.071/20 ± 6.9/50	 <i>para</i> -PhO-CHA 0.054 ± 0.0043/20 ± 6.7/370
BnO/2	 <i>ortho</i> -BnO-CHA 0.25 ± 0.068/31 ± 6.6/120	 <i>meta</i> -BnO-CHA 0.18 ± 0.066/6.6 ± 1.7/37	 <i>para</i> -BnO-CHA 0.042 ± 0.0083/9.9 ± 2.7/240
PHEO/3	 <i>ortho</i> -PHEO-CHA 0.32 ± 0.065/83 ± 2.5/260	 <i>meta</i> -PHEO-CHA 0.30 ± 0.090/12 ± 1.6/41	 <i>para</i> -PHEO-CHA 0.13 ± 0.032/16 ± 2.8/120
PEGO/4	 <i>ortho</i> -PEGO-CHA 0.37 ± 0.022/45 ± 15/120	 <i>meta</i> -PEGO-CHA 0.11 ± 0.033/6.0 ± 1.2/55	 <i>para</i> -PEGO-CHA 0.063 ± 0.017/5.7 ± 1.6/91

<sup>a</sup> Cells were treated with different concentrations of the compounds for 72 h, replicon inhibition and cell viability were measured as described in the Experimental Section; <sup>b</sup>R is the substituent abbreviation and L is the length of connection unit as number of atoms; <sup>c</sup>EC<sub>50</sub> and CC<sub>50</sub> are presented as the mean value and standard deviation of at least four and six independent experiments, correspondingly.

I versus antiviral activity (pEC<sub>50</sub>) as well as cytotoxicity (pCC<sub>50</sub>) allows to answer an important question: in the presence of which CHAs the inhibition of class I HDACs predominantly suppresses replicon propagation, and for which it mainly reduces viability of the cells.

The efficiency of inhibition of HDAC1/2/3 was initially assessed using the Western blot analysis for the content of the acetylated form of histone H3 (H3K9/14ac) in the cell lysates. The quantitative indicator of inhibition of HDAC1/2/3 was the ratio of the H3K9/14ac content to the content of unmodified histone H3 normalized to the same ratio in the absence of the inhibitor (Ac-H3/H3; Fig. 2A). To construct the corresponding scatter plots, we chose the Ac-H3/H3 values obtained at a CHA concentration of 3 μM, at which the level of H3 acetylation varied in the widest possible range (Fig. 2B, C).

The statistical relationship between the accumulation of H3K9/14ac and the values of pEC<sub>50</sub> for the entire set of CHAs was moderate and not significant ( $r = 0.495$ ,  $P < 0.1$ ). However, for the compounds of the '5 m+2 M' group, the correlation was very strong and highly significant ( $r_m = 0.928$ ,  $P < 0.005$ ). Such correlation indicators are usually typical for a causal relationship between events; in any case, they reliably guarantee the possibility of its existence. Unexpectedly, a strong and highly significant correlation ( $r = 0.741$ ,  $P < 0.002$ ) between the values of H3K9/14ac and pCC<sub>50</sub> was observed for the entire set of compounds, which, in addition to other evidence, corroborated the correctness of the results of Western blot analysis and cell viability testing selected for the scatter plot. It is important to note that the correlation indices in

the '5 m+2 M' group ( $r_m = 0.910$ ,  $P < 0.005$ ) only slightly differed from the indices in the entire set of compounds. Thus, the inhibition of HDAC1/2/3 by CHAs was responsible for their cytotoxic effect with a high degree of reliability, while the antiviral activity was statistically associated with the inhibition of HDAC1/2/3 only in the '5 m+2 M' group of compounds.

### 2.3.2. Inhibition of HDAC6

The participation of HDAC6 in the HCV life cycle remains obscure but detectable. Earlier, using two selective HDAC6 inhibitors as an example, we showed the concurrence of the curves of replicon inhibition and accumulation of the acetylated form of  $\alpha$ -tubulin ( $\alpha$ -TubK40ac), for which HDAC6 is the main deacetylating enzyme in the cells of the test system [14,22]. Then, having at our disposal a set of 15 structurally related CHAs, we planned to reliably study the statistical relationships between HDAC6 inhibition and antiviral activity as well as the cytotoxic effect of these compounds.

The results of Western blot analysis for the content of  $\alpha$ -TubK40ac in cell lysates are presented in Fig. 3A. A quantitative indicator of the inhibition of HDAC6 was the ratio of the content of  $\alpha$ -TubK40ac to the content of unmodified  $\alpha$ -Tub normalized to the same ratio in the absence of the inhibitor (Ac-Tub/Tub; Fig. 3A). To construct the correlation dependences (Fig. 3B and C), we chose the values of Ac-Tub/Tub that were obtained at a CHA concentration of 3 μM, at which the acetylation level of  $\alpha$ -Tub varied in the widest possible range, as well as in the case of the histone H3 acetylation. Interestingly, a noticeable increase in the content of  $\alpha$ -TubK40ac during cell incubation with *ortho* derivatives of CHA was observed

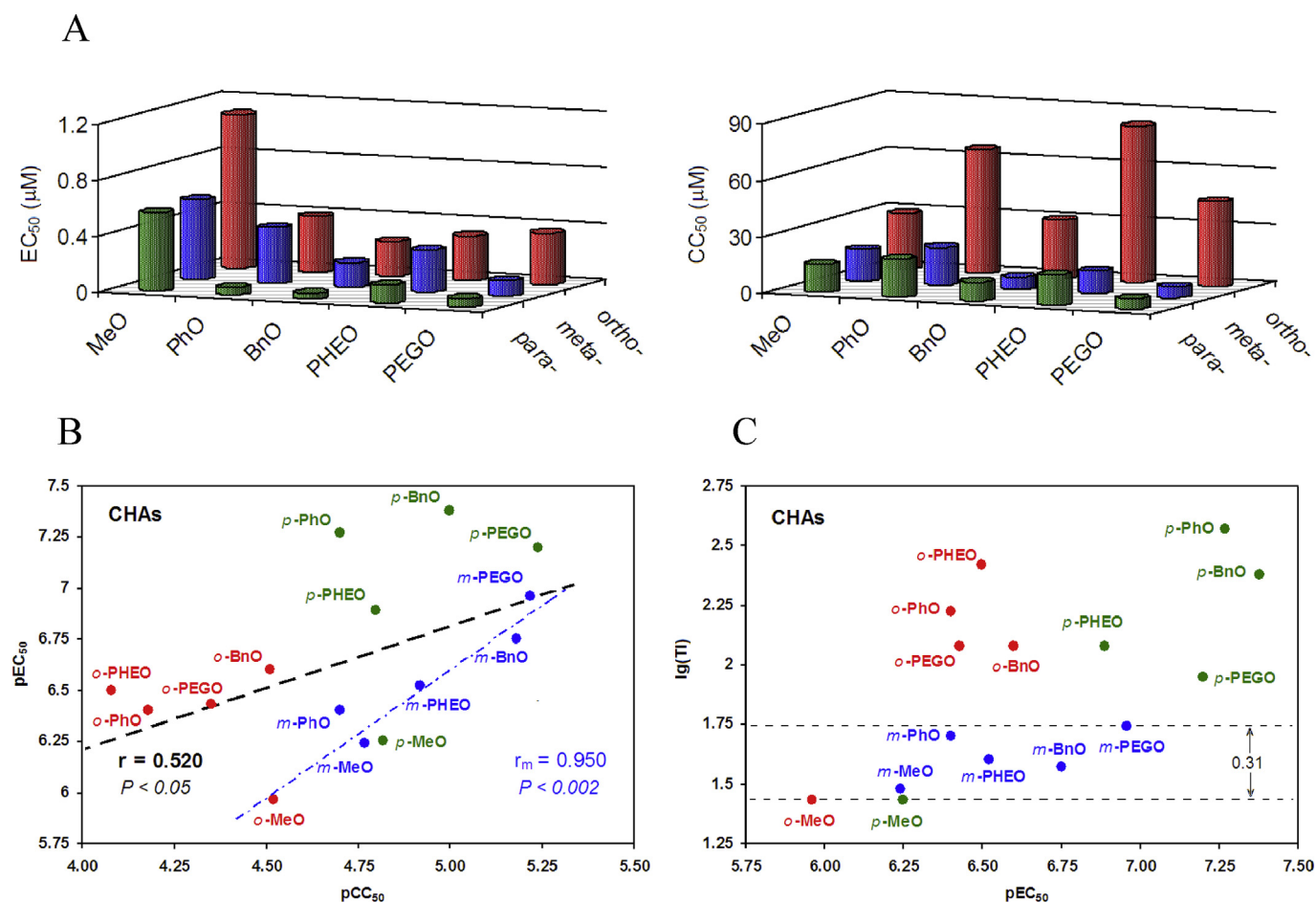


**Fig. 1.** (A) Antiviral activity ( $EC_{50}$ ) and cytotoxicity ( $CC_{50}$ ) of CHAs tested in the cell system with full-length HCV replicon. (B) Scatter plot of cytotoxicity ( $pCC_{50}$ ) versus antiviral activity ( $pEC_{50}$ );  $r$  is the correlation coefficient calculated for the full set of CHAs, and  $r_m$  is the correlation coefficient calculated for the '5 m+2 M' group of compounds (*meta*-MeO/PhO/BnO/PHEO/PEGO-CHAs plus *ortho*- and *para*-MeO-CHAs);  $P$  is the significance of the corresponding correlation. (C) Scatter plot of antiviral activity ( $pEC_{50}$ ) versus selectivity ( $\lg(TI)$ ).

only in the case of two compounds – *ortho*-MeO-CHA and *ortho*-BnO-CHA.

A moderate and insignificant correlation ( $r = 0.509$ ,  $P < 0.1$ ) between the accumulation of  $\alpha$ -TubK40ac and  $pEC_{50}$  for the entire set of CHAs became strong and increased in significance ( $r_m = 0.838$ ,  $P < 0.05$ ) for the '5 m+2 M' group of compounds. At the same time, a strong and highly significant correlation ( $r = 0.865$ ,  $P < 0.001$ ) between  $\alpha$ -TubK40ac and  $pCC_{50}$  did not fundamentally change ( $r_m = 0.919$ ,  $P < 0.005$ ) upon the transition from the entire set of compounds to the '5 m+2 M' group. Thus, the results of the SAR study of CHAs as HCV replication blockers and inhibitors of HDAC6 and HDAC1/2/3 almost completely repeated each other. As a result, we could confidently accept the inhibition of these subtypes of HDACs as the main source of the cytotoxic effect of the studied CHAs, as well as the anti-HCV activity for the '5 m+2 M' group of compounds.

### 2.3.3. Inhibition of HDAC8

The lack of correlation between the suppression of HCV replication and the inhibition of HDAC1/2/3/6 for phenyl *ortho* derivatives of CHA led us to view HDAC8 as another possible antiviral target, since it is *ortho* isomers that have an increased selectivity for HDAC8 [19]. Currently, the relationship of HDAC8 with HCV replicon propagation remains in question. In our hands, the inhibition of HCV replication with pyridyl-4-oxy *ortho* derivative of CHA, a new

selective HDAC8 inhibitor, demonstrated a positive correlation with the accumulation of the acetylated form of the protein of the cohesin complex SMC3 (SMC3K105/106ac) [22], which is a bona fide protein substrate of HDAC8 [24]. The results of Western blot analysis for the content of SMC3K105/106ac after the incubation of cells in the presence of phenyl *ortho*, *meta* and *para* derivatives of CHA are presented in Fig. 4A. As expected, which was nevertheless surprising, the inhibition of HDAC8 with CHAs even at high concentrations took place only in the case of *ortho* derivatives, with one exception of *m*-PEGO-CHA at 10  $\mu$ M concentration.

To compare the curves of HCV replication suppression and HDAC8 inhibition, the accumulation of SMC3K105/106ac in cells after their treatment with *ortho*-CHAs was additionally measured at concentrations of 0.1, 0.3 and 1  $\mu$ M (Fig. 4A). As shown in Fig. 4B, the WB signal was noticeable, starting from 0.1  $\mu$ M concentration of all *ortho*-CHAs, and then increased in parallel with the suppression of HCV replication, and only in the case of *o*-BnO-CHA, the replicon inhibition was significantly outpacing the accumulation of SMC3K105/106ac. Interestingly, in contrast to other *ortho* derivatives, *o*-BnO-CHA inhibited both HDAC1/2/3 and HDAC6; perhaps, it was the polypotent effect of this compound that caused the observed 'gap effect'.

Using all data obtained (24 pairs of values), we built a scatter plot of logarithm of the normalized ratio of Ac-SMC3/SMC3 versus replicon inhibition and calculated the corresponding correlation

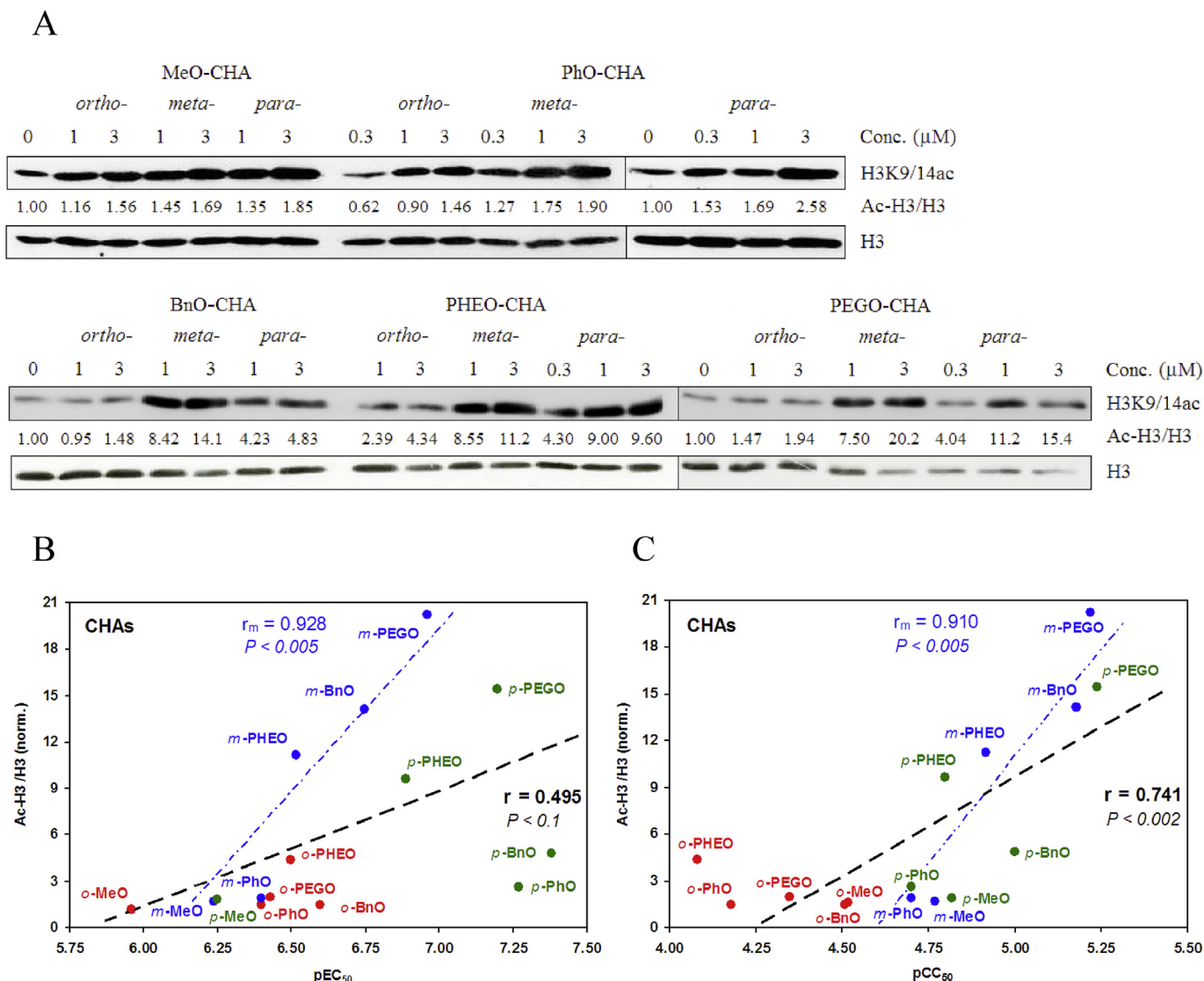


**Fig. 2.** (A) Western blot analysis for the content of the acetylated forms of histone H3 (H3K9/14ac) in Huh7-luc/neo cells treated with CHAs for 24 h. (B and C) Scatter plots of the values of  $pEC_{50}$  and  $pCC_{50}$  versus the relative content of H3K9/14ac in the presence of 3  $\mu$ M CHAs;  $r$  is the correlation coefficient calculated for the entire set of CHAs and  $r_m$  is the correlation coefficient, calculated for the '5 m+2 M' group of compounds;  $P$  is the significance of the corresponding correlation.

coefficient, the value of which with very high reliability ( $r = 0.832$ ,  $P < 0.001$ ) corroborated the existence of a strong statistical relationship between inhibition of HDAC8 and anti-HCV activity of *ortho*-CHAs (Fig. 4C).

#### 2.4. Independent antiviral effect of *para*-CHAs on HDACs

All the results obtained in this work indicated that the antiviral activity of phenyl *para* derivatives of CHA can not be interpreted as a result of the inhibition of HDACs class I/IIb. This can be visually demonstrated using the graphs of the concentration dependence of HCV replication suppression and accumulation of H3K9/14ac and  $\alpha$ -TubK40ac for each of the *para*-CHAs (Fig. 5). It can be seen that in the presence of 0.3  $\mu$ M of any of the compounds, 80–90% inhibition of the replicon was already taking place, while the level of acetylation of protein substrates was only beginning to grow, and neither the rate of this growth nor the maximum achievable values correlated with the corresponding values of  $EC_{50}$ .

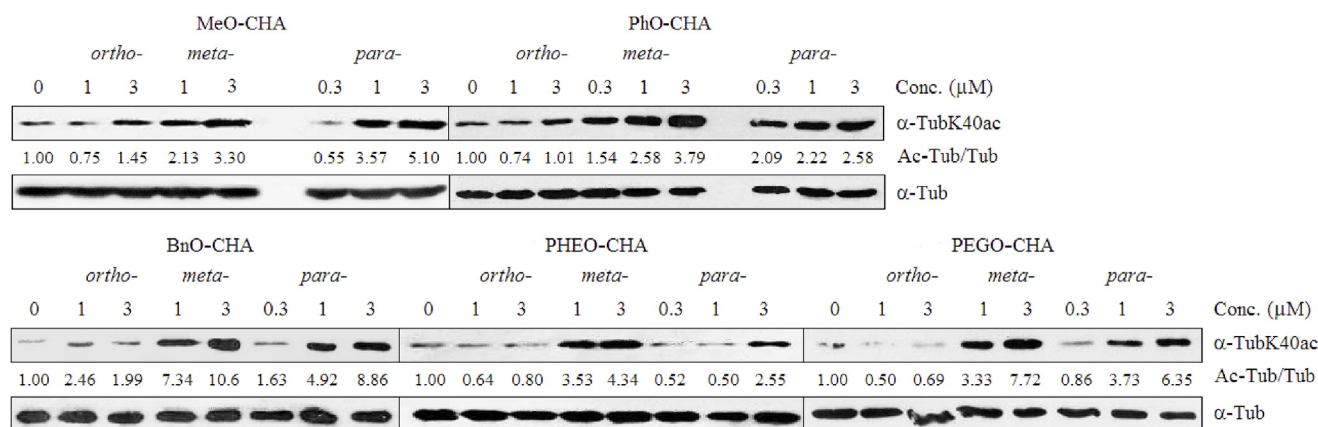
Most likely, the inhibition of HDAC1/2/3/6 with *para*-CHAs upon reaching the concentration of 0.3  $\mu$ M and higher contributes to the

suppression of HCV replication. However, in order to demonstrate the  $EC_{50}$  values at the level of 40–60 nM concentrations, *para*-CHAs should probably inhibit a more susceptible antiviral target X, which does not belong to the studied group of HDACs. This assumption explains rather well why phenyl *meta* derivatives of CHA as well as methoxy derivatives of CHA showed similar patterns of anti-HCV action, forming a separate group of compounds '5 m+2 M' (Figs. 1–3). Indeed, since the phenyl *meta* derivatives of CHA did not have the required molecular geometry, while the methoxy derivatives of CHA did not contain an aromatic substituent at all, all of these compounds were unable to inhibit either HDAC8 targeted by *ortho*-CHAs or hypothetical target X for *para*-CHAs, but exclusively HDAC1/2/3/6.

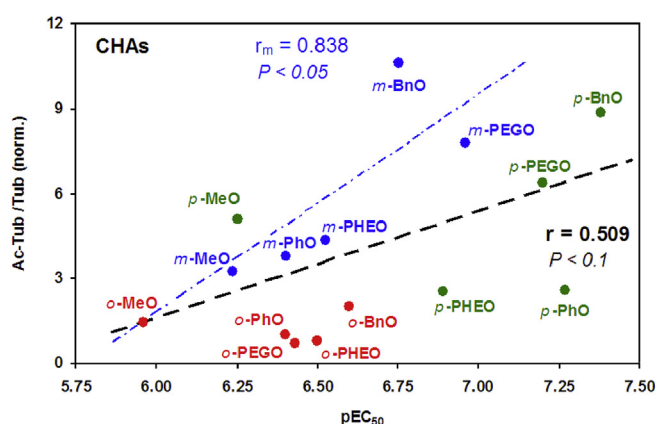
### 3. Conclusion

Using a set of structural isomers of CHA carrying a phenyl substituent in the aromatic ring of a cinnamic acid residue, we were able to establish statistical relationships between inhibition of HDACs class I/IIb and suppression of HCV replicon propagation.

A



B



C

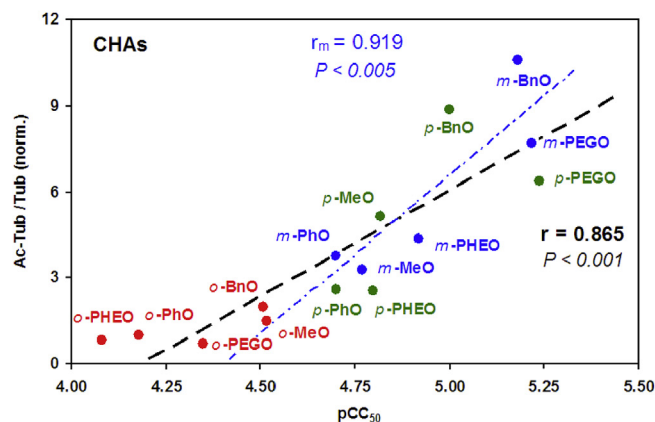


**Fig. 3.** (A) Western blot analysis for the content of the acetylated form of  $\alpha$ -tubulin ( $\alpha$ -TubK40ac) in Huh7-luc/neo cells treated with CHAs for 24 h. (B and C) Scatter plots of the values of  $pEC_{50}$  and  $pCC_{50}$  versus the relative content of  $\alpha$ -TubK40ac in the presence of 3  $\mu$ M CHA;  $r$  is the correlation coefficient calculated for the entire set of CHAs and  $r_m$  is the correlation coefficient, calculated for the '5 m+2 M' group of compounds;  $P$  is the significance of the corresponding correlation.

Anti-HCV activity correlated strongly and significantly with the inhibition of HDAC8 in the case of *ortho*-CHAs, while in the case of *meta*-CHAs it correlated in a similar manner with the inhibition of HDAC1/2/3 and HDAC6. The antiviral activity of *para*-CHAs was many times stronger than that of *meta*-CHAs, despite about the same efficiency of HDAC1/2/3/6 inhibition. Based on this observation, we suggested the existence of an additional antiviral target, the identification of which is of unquestionable interest. Finally, the results of the SAR study will be useful for the design of new derivatives of cinnamic hydroxamic acid – host targeting agents that suppress HCV replication.

## 4. Experimental section

### 4.1. Chemistry

#### 4.1.1. General

NMR spectra ( $\delta$ , ppm;  $J$ , Hz) were registered on a AMX III-400 spectrometer (Bruker, Germany) at 400 MHz for  $^1\text{H}$  NMR (internal standard:  $\text{Me}_4\text{Si}$ ; solvent:  $\text{DMSO}-d_6$ ) and 100.6 MHz for  $^{13}\text{C}$  NMR with suppression of carbon-proton interaction (solvent:  $\text{DMSO}-d_6$ ). High-resolution mass spectra (HRMS) were registered on a Bruker

Daltonics microTOF-Q II hybrid quadrupole time-of-flight mass spectrometer using electrospray ionization (ESI); measurements were done in positive ion mode. Cinnamic acids formed stable complexes of association ions with potassium impurity ions [25], which were observed as an overlaid sharp peak on the base peak chromatogram. TLC was performed on the plates of Kieselgel 60 F254 (Merck) and the column chromatography was carried out on silica gel (Kieselgel, 0.035–0.070 mm, Acros Organics) using the elution systems mentioned in the text.

#### 4.1.2. Synthesis of *ortho*-, *meta*- and *para*-MeO-CHA

(iii) To a solution of the corresponding acid (0.71 g, 4.0 mmol) in DMF (4 ml), CDI (0.65 g, 4.0 mmol) was added. After 2 h incubation,  $\text{NH}_2\text{OH}\cdot\text{HCl}$  (0.56 g, 8.0 mmol) was added, the mixture was stirred for 15 min and kept overnight (~18 h). Vessel contents were mixed with *o*-xylol (8 ml) and evaporated. The residue was dissolved in EtOAc (25 ml) and washed with 4%  $\text{NaHCO}_3$  (25 ml) followed by  $\text{H}_2\text{O}$  (25 ml), dried over  $\text{Na}_2\text{SO}_4$  and evaporated. The product was isolated by silica gel chromatography using a  $\text{CHCl}_3$ –EtOH–AcOH mixture (100 : 10 : 1) as an eluent. The selected fractions were evaporated, the crude

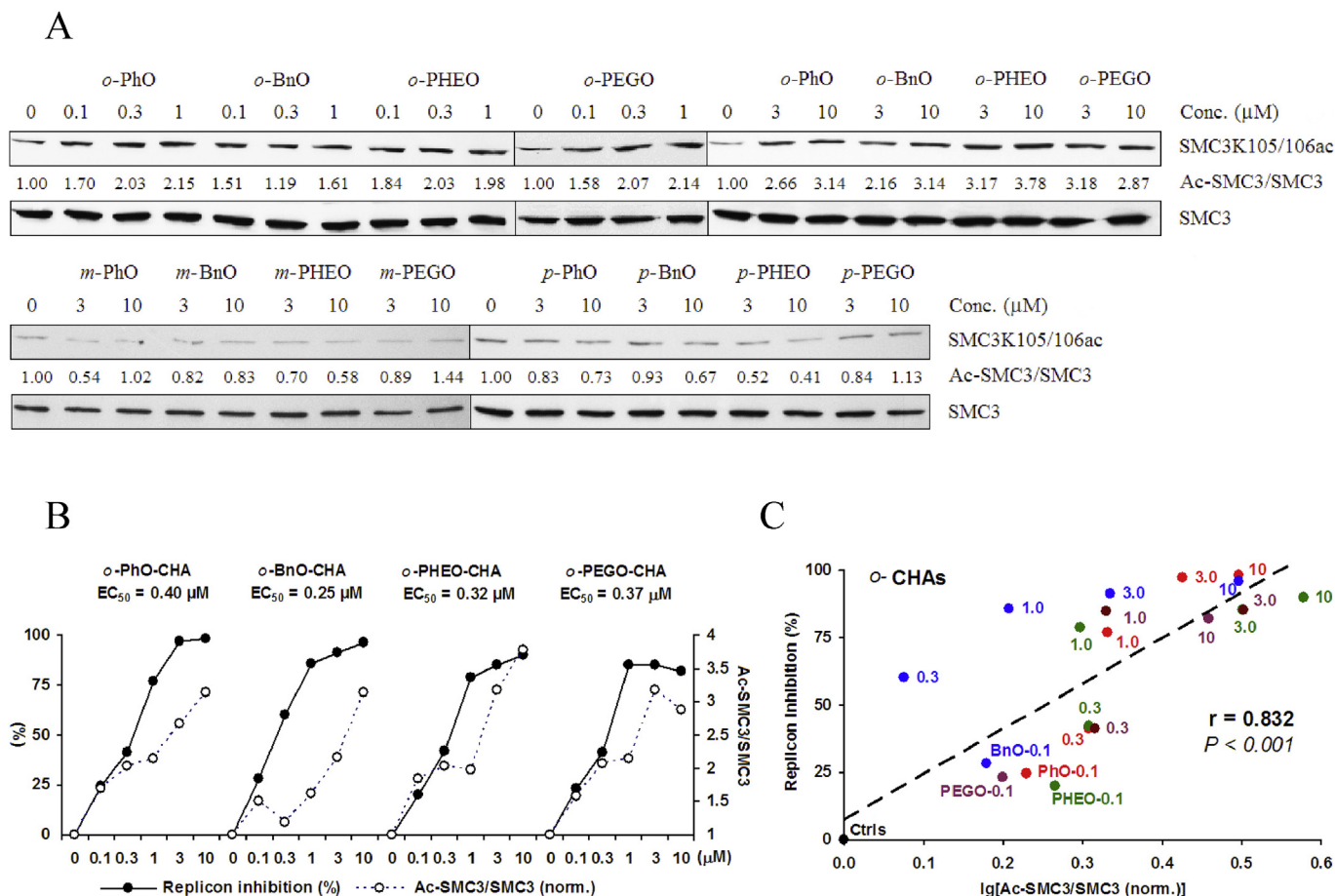


**Fig. 4.** (A) Western blot analysis for the content of the acetylated forms of SMC3 (SMC3K105/106ac) in Huh7-luc/neo cells treated with CHAs for 24 h. (B) The relationship between inhibition of HDAC8 and HCV replication blocking with CHAs; inhibition of the replicon for 72 h is expressed as a percentage (left axis); the values of HDAC8 inhibition were calculated as the Ac-SMC3/SMC3 normalized ratio (right axis). (C) Scatter plot of logarithm of the relative content of SMC3K105/106ac (in the presence of 0, 0.1, 0.3, 1, 3 and 10  $\mu\text{M}$  of *ortho*-PhO/BnO/PHEO/PEGO-CHAs for 24 h) versus replicon inhibition (%);  $r$  and  $P$  are the correlation coefficient and its significance.

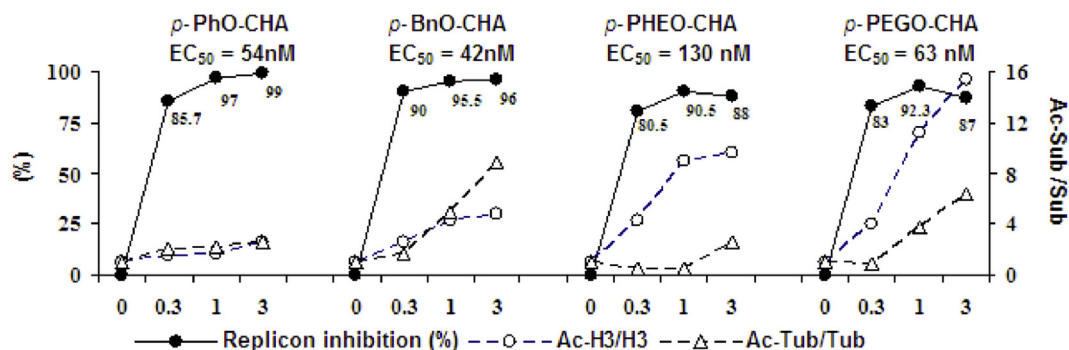


**Fig. 5.** The relationship between the inhibition of HDAC1/2/3/6 and HCV replication blocking with *para*-CHAs; the replicon inhibition for 72 h is expressed as a percentage (left axis); the values of HDAC1/2/3 and HDAC6 inhibition for 24 h were calculated as the Ac-H3/H3 and Ac-Tub/Tub normalized ratios (right axis).

product was washed with a small volume of non-polar solvent (benzene, 1,2-DCE or  $\text{CHCl}_3$ ), the obtained precipitate was filtered and air dried. The yields of *ortho*-, *meta*- and *para*-MeO-CHA were 19, 25 and 40%, respectively.

(*E*)-*N*-Hydroxy-3-(2-methoxyphenyl)acrylamide (*ortho*-MeO-CHA):  $^1\text{H}$  NMR (400 MHz, DMSO)  $\delta$  10.69 (s, 1H), 8.95 (s, 1H), 7.68 (d,  $J = 15.8$  Hz, 1H), 7.50 (d,  $J = 7.9$  Hz, 1H), 7.36 (t,  $J = 7.8$  Hz, 1H), 7.07 (d,  $J = 8.1$  Hz, 1H), 6.98 (t,  $J = 7.5$  Hz, 1H), 6.50 (d,  $J = 16.0$  Hz,

1H), 3.86 (s, 3H).  $^{13}\text{C}$  NMR (75 MHz, DMSO- $d_6$ )  $\delta$  163.66, 157.99, 133.84, 131.28, 128.32, 123.68, 121.16, 119.91, 112.17, 56.02. ESI-HRMS  $m/z$ : Calcd for  $\text{C}_{10}\text{H}_{11}\text{NO}_3$   $[\text{M}+\text{H}]^+$  194.0812, found 194.0816; calcd  $[\text{M}+\text{Na}]^+$  216.0631, found 216.0638.

(*E*)-*N*-Hydroxy-3-(3-methoxyphenyl)acrylamide (*meta*-MeO-CHA):  $^1\text{H}$  NMR (400 MHz, DMSO)  $\delta$  10.78 (s, 1H), 9.10 (bs, 1H), 7.42 (d,  $J = 15.8$  Hz, 1H), 7.31 (t,  $J = 7.9$  Hz, 1H), 7.17–7.06 (m, 2H), 6.94 (d,  $J = 6.6$  Hz, 1H), 6.50 (d,  $J = 15.8$  Hz, 1H), 3.78 (s, 3H).  $^{13}\text{C}$  NMR (101 MHz, DMSO)  $\delta$  162.66, 159.56, 138.16, 136.25, 129.89, 119.71,

119.49, 115.16, 112.63, 55.08. ESI-HRMS  $m/z$ : Calcd for  $C_{10}H_{11}NO_3$   $[M+H]^+$  194.0812, found 194.0808; calcd  $[2 M + H]^+$  387.1551, found 387.1550.

(*E*)-*N*-Hydroxy-3-(4-methoxyphenyl)acrylamide (*para*-MeO-CHA):  $^1H$  NMR (400 MHz, DMSO)  $\delta$  9.78 (bs, 2H), 7.48 (d,  $J = 8.3$  Hz, 2H), 7.33 (d,  $J = 15.8$  Hz, 1H), 6.95 (d,  $J = 8.6$  Hz, 2H), 6.31 (d,  $J = 15.9$  Hz, 1H), 3.78 (s, 3H).  $^{13}C$  NMR (75 MHz, DMSO- $d_6$ )  $\delta$  163.60, 160.64, 137.78, 129.40, 128.08, 117.5, 114.80, 55.70. ESI-HRMS  $m/z$ : Calcd for  $C_{10}H_{11}NO_3$   $[M+H]^+$  194.0812, found 194.0813; calcd  $[2 M + H]^+$  387.1551, found 387.1558.

#### 4.1.3. Synthesis of *ortho*-, *meta*- and *para*-PhO-CHA

(iii) To a solution of the corresponding acid (0.72 g, 3.0 mmol) in DMF (3 ml), CDI (0.50 g, 3.0 mmol) was added. After 2 h incubation,  $NH_2OH \cdot HCl$  (0.21 g, 3.0 mmol) was added, the mixture was stirred for 15 min and kept overnight (~18 h). The solution was poured into  $H_2O$  (25 ml) and washed with EtOAc (25 ml); the organic layer was washed with  $H_2O$  (20 ml), dried over  $Na_2SO_4$  and evaporated. The *o*- and *m*-PhOCHA or *p*-PhOCHA were isolated by silica gel chromatography using EtOAc or a  $CHCl_3$ -EtOH-AcOH mixture (100 : 10: 1) as eluents, correspondingly. The selected fractions were evaporated, the crude product was washed with a small volume of non-polar solvent (1,2-DCE or  $CCl_4$ ), the obtained precipitate was filtered and air dried. The yields of *o*-, *m*- and *p*-PhO-CHA were 20, 28 and 21%, respectively.

(*E*)-*N*-Hydroxy-3-(2-phenoxyphenyl)acrylamide (*ortho*-PhO-CHA):  $^1H$  NMR (400 MHz, DMSO- $d_6$ )  $\delta$  10.80 (s, 1H), 9.04 (s, 1H), 7.75–7.57 (m, 2H), 7.38 (bs, 3H), 7.21 (bs, 1H), 7.13 (bs, 1H), 6.99–6.95 (m, 2H), 6.91 (d,  $J = 7.2$  Hz, 2H), 6.57 (d,  $J = 15.5$  Hz, 1H).  $^{13}C$  NMR (101 MHz, DMSO)  $\delta$  162.64, 156.81, 154.47, 132.28, 130.97, 130.10, 128.07, 126.37, 124.30, 123.40, 120.74, 119.55, 118.02. ESI-HRMS ( $m/z$ ): Calcd for  $C_{15}H_{13}NO_3$   $[M+H]^+$  256.0968, found 256.0968; calcd  $[M+Na]^+$  278.0788, found 278.0788.

(*E*)-*N*-Hydroxy-3-(3-phenoxyphenyl)acrylamide (*meta*-PhO-CHA):  $^1H$  NMR (400 MHz, DMSO)  $\delta$  10.71 (bs, 1H), 9.04 (bs, 1H), 7.46–7.36 (m, 4H), 7.33 (d,  $J = 7.3$  Hz, 1H), 7.23–7.11 (m, 2H), 7.02 (dd,  $J = 15.5$ , 7.7 Hz, 3H), 6.43 (d,  $J = 15.8$  Hz, 1H).  $^{13}C$  NMR (101 MHz, DMSO- $d_6$ )  $\delta$  162.39, 157.11, 156.33, 137.50, 136.86, 130.50, 130.05, 123.62, 122.73, 119.99, 119.44, 118.71, 116.88. ESI-HRMS ( $m/z$ ): Calcd for  $C_{15}H_{13}NO_3$   $[M+H]^+$  256.0968, found 256.0969; calcd  $[M+Na]^+$  278.0788, found 278.0788.

(*E*)-*N*-Hydroxy-3-(4-phenoxyphenyl)acrylamide (*para*-PhO-CHA):  $^1H$  NMR (400 MHz, DMSO)  $\delta$  10.70 (bs, 1H), 8.99 b(s, 1H), 7.57 (d,  $J = 8.2$  Hz, 2H), 7.49–7.38 (m, 3H), 7.18 (t,  $J = 7.4$  Hz, 1H), 7.06 (d,  $J = 7.9$  Hz, 2H), 7.00 (d,  $J = 8.6$  Hz, 2H), 6.38 (d,  $J = 15.8$  Hz, 1H).  $^{13}C$  NMR (101 MHz, DMSO)  $\delta$  162.79, 157.82, 155.87, 137.49, 130.07, 129.90, 129.25, 123.92, 119.11, 118.38, 117.95. ESI-HRMS ( $m/z$ ): Calcd for  $C_{15}H_{13}NO_3$   $[M+H]^+$  256.0968, found 256.0973.

(ii) Preparation of *ortho*-, *meta*- and *para*-PhO-CA. To the mixture of the corresponding aldehyde (2.52 g, 12.7 mmol) and malonic acid (1.99 g, 19.1 mmol), dry pyridine (6.5 ml) and piperidine (0.2 ml) were successively added. The mixture was stirred at 120 °C for 3 h, cooled to 10 °C and acidified with HCl (~14 ml) at 1:1 ratio with cooling and stirring. After 30 min, the precipitate was filtered, washed 3 times with  $H_2O$  (20 ml) and air dried. The yields of *o*-, *m*- and *p*-PhO-CA were 92, 91 and 96%, respectively.

(*E*)-3-(2-Phenoxyphenyl)acrylic acid (*ortho*-PhO-CA):  $^1H$  NMR (400 MHz, DMSO)  $\delta$  12.44 (s, 1H), 7.89 (dd,  $J = 7.8$ , 1.2 Hz, 1H), 7.79 (d,  $J = 16.2$  Hz, 1H), 7.46–7.35 (m, 3H), 7.21 (t,  $J = 7.5$  Hz, 1H), 7.15 (t,  $J = 7.4$  Hz, 1H), 6.98 (d,  $J = 7.8$  Hz, 2H), 6.92 (d,  $J = 8.1$  Hz, 1H), 6.60 (d,  $J = 16.1$  Hz, 1H).  $^{13}C$  NMR (101 MHz, DMSO)  $\delta$  167.48, 156.73, 154.72, 137.50, 131.86, 130.16, 128.57, 125.62, 124.26, 123.54, 120.61,

119.41, 118.06. ESI-HRMS ( $m/z$ ): Calcd for  $C_{15}H_{12}O_3$   $[M+H]^+$  241.0859, found 241.0861; calcd  $[M + NH_4]^+$  258.1125, found 258.1128; calculated  $[M+Na]^+$  263.0679, found 263.0683; calcd  $[6 M + K]^+$  740.2212, found 740.2166; calcd  $[6 M + K]^+$  1479.4350, found 1479.4278.

(*E*)-3-(3-Phenoxyphenyl)acrylic acid (*meta*-PhO-CA):  $^1H$  NMR (400 MHz, DMSO)  $\delta$  12.41 (bs, 1H), 7.57 (d,  $J = 16.0$  Hz, 1H), 7.49–7.34 (m, 5H), 7.15 (t,  $J = 7.4$  Hz, 1H), 7.06–6.96 (m, 3H), 6.51 (d,  $J = 16.0$  Hz, 1H).  $^{13}C$  NMR (101 MHz, DMSO)  $\delta$  167.30, 157.01, 156.40, 143.05, 136.29, 130.42, 130.01, 123.54, 123.26, 120.14, 120.10, 118.60, 118.13. ESI-HRMS ( $m/z$ ): Calcd for  $C_{15}H_{12}O_3$   $[M+H]^+$  241.0859, found 241.0864; calcd  $[5 M + K]^{2+}$  620.1818, found 620.1772; calcd  $[6 M + K]^{2+}$  740.2212, found 740.2179; calcd  $[4 M + K]^+$  999.2777, found 999.2716. calcd  $[5 M + K]^+$  1239.3564, found 1239.3512.

(*E*)-3-(4-Phenoxyphenyl)acrylic acid (*para*-PhO-CA):  $^1H$  NMR (400 MHz, DMSO)  $\delta$  12.30 (bs, 1H), 7.70 (d,  $J = 8.7$  Hz, 2H), 7.58 (d,  $J = 16.0$  Hz, 1H), 7.42 (t,  $J = 8.0$  Hz, 2H), 7.19 (t,  $J = 7.4$  Hz, 1H), 7.07 (d,  $J = 7.7$  Hz, 2H), 6.99 (d,  $J = 8.7$  Hz, 2H), 6.44 (d,  $J = 16.0$  Hz, 1H).  $^{13}C$  NMR (101 MHz, DMSO- $d_6$ )  $\delta$  167.56, 158.58, 155.67, 143.12, 130.12, 129.23, 124.11, 119.32, 118.17, 117.96. ESI-HRMS ( $m/z$ ): Calcd for  $C_{15}H_{12}O_3$   $[M+H]^+$  241.0859, found 241.0864; calcd  $[5 M + K]^{2+}$  620.1818, found 620.1779; calcd  $[6 M + K]^{2+}$  740.2212, found 740.2181; calcd  $[4 M + K]^+$  999.2777, found 999.2722.

#### 4.1.4. Synthesis of *ortho*-, *meta*- and *para*-BnO-CHA

(iii) To a solution of the corresponding acid (0.51 g, 2.0 mmol) in DMF (2 ml), CDI (0.33 g, 2.0 mmol) was added. After 2 h incubation,  $NH_2OH \cdot HCl$  (0.16 g, 2.3 mmol) was added, the mixture was stirred for 15 min and kept overnight (~18 h). The solution was poured into  $H_2O$  (20 ml) and the product was isolated from oily residue by silica gel chromatography using a  $CHCl_3$ -EtOH mixture (100 : 10) as an eluent. The selected fractions were evaporated, the crude product was washed with a small volume of non-polar or low polar solvents (1,2-DCE, MeCN or EtOH), the obtained precipitate was filtered and air dried. The yields of *o*-, *m*- and *p*-BnO-CHA were 26, 22 and 17%, respectively.

(*E*)-3-(2-(Benzyloxy)phenyl)-*N*-hydroxyacrylamide (*ortho*-BnO-CHA):  $^1H$  NMR (400 MHz, DMSO)  $\delta$  10.72 (bs, 1H), 9.00 (bs, 1H), 7.77 (d,  $J = 15.9$  Hz, 1H), 7.53 (d,  $J = 7.2$  Hz, 1H), 7.49–7.28 (m, 6H), 7.14 (d,  $J = 8.2$  Hz, 1H), 6.98 (t,  $J = 7.3$  Hz, 1H), 6.50 (d,  $J = 15.9$  Hz, 1H), 5.21 (s, 2H).  $^{13}C$  NMR (101 MHz, DMSO)  $\delta$  163.04, 156.31, 136.85, 133.01, 130.67, 128.48, 127.85, 127.46, 123.67, 120.92, 119.42, 113.12, 69.55. ESI-HRMS ( $m/z$ ): Calcd for  $C_{16}H_{15}NO_3$   $[M+H]^+$  270.1125, found 270.1125; calcd  $[M+Na]^+$  292.0944, found 292.0948.

(*E*)-3-(3-(Benzyloxy)phenyl)-*N*-hydroxyacrylamide (*meta*-BnO-CHA):  $^1H$  NMR (400 MHz, DMSO- $d_6$ )  $\delta$  9.92 (bs, 1H), 7.51–7.36 (m, 5H), 7.36–7.28 (m, 2H), 7.21 (s, 1H), 7.14 (d,  $J = 7.5$  Hz, 1H), 7.02 (d,  $J = 8.1$  Hz, 1H), 6.48 (d,  $J = 15.8$  Hz, 1H), 5.14 (s, 2H).  $^{13}C$  NMR (101 MHz, DMSO- $d_6$ )  $\delta$  162.52, 158.63, 137.89, 136.88, 136.30, 129.91, 128.37, 127.79, 127.66, 119.89, 119.55, 115.92, 113.58, 69.18. ESI-HRMS ( $m/z$ ): Calcd for  $C_{16}H_{15}NO_3$   $[M+H]^+$  270.1125, found 270.1125; calcd  $[M+Na]^+$  292.0944, found 292.0944.

(*E*)-3-(4-(Benzyloxy)phenyl)-*N*-hydroxyacrylamide (*para*-BnO-CHA):  $^1H$  NMR (400 MHz, DMSO)  $\delta$  10.64 (bs, 1H), 8.95 (bs, 1H), 7.50 (d,  $J = 8.2$  Hz, 2H), 7.47–7.30 (m, 6H), 7.04 (d,  $J = 8.6$  Hz, 2H), 6.32 (d,  $J = 15.7$  Hz, 1H), 5.14 (s, 2H).  $^{13}C$  NMR (101 MHz, DMSO)  $\delta$  163.07, 159.31, 137.89, 136.73, 128.95128.36, 127.80, 127.61, 116.61, 115.15, 69.25. ESI-HRMS ( $m/z$ ): Calcd for  $C_{16}H_{15}NO_3$   $[M+H]^+$  270.1125; found 270.1128; calcd  $[M+Na]^+$  292.0944, found 292.0948.

(ii) Preparation of *ortho*-, *meta*- and *para*-BnO-CA was performed exactly as described for PhO-CA in section 4.1.3. The yields of the corresponding structural isomers were 87, 96 and 94%.

(*E*)-3-(2-(Benzyloxy)phenyl)acrylic acid (*ortho*-BnO-CA):  $^1H$  NMR

(400 MHz, DMSO)  $\delta$  12.27 (bs, 1H), 7.89 (d,  $J = 16.2$  Hz, 1H), 7.69 (dd,  $J = 7.7, 1.4$  Hz, 1H), 7.51–7.31 (m, 6H), 7.17 (d,  $J = 8.4$  Hz, 1H), 6.99 (t,  $J = 7.5$  Hz, 1H), 6.53 (d,  $J = 16.2$  Hz, 1H), 5.21 (s, 2H).  $^{13}\text{C}$  NMR (101 MHz, DMSO)  $\delta$  167.74, 156.71, 138.59, 136.69, 131.56, 128.47, 127.92, 127.57, 122.83, 120.92, 119.38, 113.06, 69.71. ESI-HRMS ( $m/z$ ): Calcd for  $\text{C}_{16}\text{H}_{14}\text{O}_3$   $[\text{M}+\text{H}]^+$  255.1016, found 255.1016; calcd  $[\text{M} + \text{NH}_4]^+$  272.1281, found 272.1281; calcd  $[\text{M}+\text{Na}]^+$  277.0835, found 277.0833; calcd  $[2\text{M} + \text{Na}]^+$  531.1778, found 531.1781; calcd  $[6\text{M} + \text{K}]^{2+}$  782.2681, found 782.2624; calcd  $[7\text{M} + \text{K}]^{2+}$  909.3152, found 909.3092; calcd  $[5\text{M} + \text{K}]^+$  1309.4346, found 1309.4241; calcd  $[6\text{M} + \text{K}]^+$  1563.5289, found 1563.5204.

(*E*)-3-(3-(Benzyloxy)phenyl)acrylic acid (*meta*-BnO-CA):  $^1\text{H}$  NMR (400 MHz, DMSO)  $\delta$  12.37 (s, 1H), 7.56 (d,  $J = 16.0$  Hz, 1H), 7.47 (d,  $J = 7.3$  Hz, 2H), 7.44–7.29 (m, 5H), 7.25 (d,  $J = 7.6$  Hz, 1H), 7.06 (dd,  $J = 8.1, 1.7$  Hz, 1H), 6.55 (d,  $J = 16.0$  Hz, 1H), 5.15 (s, 2H).  $^{13}\text{C}$  NMR (101 MHz, DMSO- $d_6$ )  $\delta$  167.45, 158.64, 143.72, 136.89, 135.63, 129.88, 128.35, 127.77, 127.67, 120.95, 119.56, 116.98, 113.76, 69.26. ESI-HRMS ( $m/z$ ): Calcd for  $\text{C}_{16}\text{H}_{14}\text{O}_3$   $[\text{M}+\text{H}]^+$  255.1016, found 255.1018; calcd  $[\text{M}+\text{Na}]^+$  277.0835, found 277.0833; calcd  $[6\text{M} + \text{K}]^{2+}$  782.2681, found 782.2629; calcd  $[7\text{M} + \text{K}]^{2+}$  909.3152, found 909.3104; calcd  $[8\text{M} + \text{K}]^{2+}$  1036.3624, found 1036.3564; calcd  $[5\text{M} + \text{K}]^+$  1309.4346, found 1309.4249.

(*E*)-3-(4-(Benzyloxy)phenyl)acrylic acid (*para*-BnO-CA):  $^1\text{H}$  NMR (400 MHz, DMSO- $d_6$ )  $\delta$  12.19 (s, 1H), 7.62 (d,  $J = 8.7$  Hz, 2H), 7.55 (d,  $J = 16.0$  Hz, 1H), 7.45 (d,  $J = 7.3$  Hz, 2H), 7.39 (t,  $J = 7.3$  Hz, 2H), 7.33 (dd,  $J = 8.4, 5.9$  Hz, 1H), 7.04 (d,  $J = 8.7$  Hz, 2H), 6.38 (d,  $J = 16.0$  Hz, 1H), 5.15 (s, 2H).  $^{13}\text{C}$  NMR (101 MHz, DMSO- $d_6$ )  $\delta$  167.72, 159.96, 143.59, 136.69, 129.84, 128.39, 127.84, 127.64, 127.01, 116.62, 115.15, 69.31. ESI-HRMS ( $m/z$ ): Calcd for  $\text{C}_{16}\text{H}_{14}\text{O}_3$   $[\text{M}+\text{H}]^+$  255.1016, found 255.1016; calcd  $[\text{M}+\text{Na}]^+$  277.0835, found 277.0833; calcd  $[2\text{M} + \text{Na}]^+$  531.1778, found 531.1780; calcd  $[6\text{M} + \text{K}]^{2+}$  782.2681, found 782.2632; calcd  $[7\text{M} + \text{K}]^{2+}$  909.3152, found 909.3067; calcd  $[4\text{M} + \text{K}]^+$  1055.3403, found 1055.3341; calcd  $[5\text{M} + \text{K}]^+$  1309.4346, found 1309.4210.

#### 4.1.5. Synthesis of *ortho*-, *meta*- and *para*-PHEO-CHA

(iii) To a solution of the corresponding acid (0.80 g, 3.0 mmol) in DMF (3 ml), CDI (0.50 g, 3.0 mmol) was added. After 2 h incubation,  $\text{NH}_2\text{OH}\cdot\text{HCl}$  (0.21 g, 3.0 mmol) was added, the mixture was stirred for 15 min and kept overnight (~18 h). The solution was diluted with 10%  $\text{KHCO}_3$  (25 ml) and washed with a mixture of EtOAc (30 ml) and MeOH (8 ml). Organic layer was filtered, washed with brine (15 ml), dried over  $\text{Na}_2\text{SO}_4$  and evaporated. The product was isolated by silica gel chromatography using a  $\text{CHCl}_3$ –EtOH mixture (10 : 1) as an eluent. The selected fractions were evaporated, the crude product was washed with a small volume of non-polar solvent (toluene or  $\text{CCl}_4$ ), the obtained precipitate was filtered and air dried. The yields of *o*-, *m*- and *p*-PHEO-CHA were 22, 25 and 20%, respectively.

(*E*)-*N*-Hydroxy-3-(2-phenethoxyphenyl)acrylamide (*ortho*-PHEO-CHA):  $^1\text{H}$  NMR (400 MHz, DMSO)  $\delta$  10.73 (bs, 1H), 9.00 (bs, 1H), 7.71 (d,  $J = 15.9$  Hz, 1H), 7.49 (d,  $J = 7.3$  Hz, 1H), 7.40–7.27 (m, 5H), 7.21 (t,  $J = 7.1$  Hz, 1H), 7.06 (d,  $J = 8.3$  Hz, 1H), 6.95 (t,  $J = 7.4$  Hz, 1H), 6.52 (d,  $J = 15.9$  Hz, 1H), 4.24 (t,  $J = 6.8$  Hz, 2H), 3.11 (t,  $J = 6.7$  Hz, 2H).  $^{13}\text{C}$  NMR (101 MHz, DMSO)  $\delta$  163.18, 156.66, 138.28, 133.49, 130.71, 129.03, 128.26, 127.94, 126.25, 123.32, 120.66, 119.46, 112.47, 68.77, 34.97. ESI-HRMS ( $m/z$ ): Calcd for  $\text{C}_{17}\text{H}_{17}\text{NO}_3$   $[\text{M}+\text{H}]^+$  284.1281, found 284.1281; calcd  $[\text{M}+\text{Na}]^+$  306.1101, found 306.1101.

(*E*)-*N*-Hydroxy-3-(3-phenethoxyphenyl)acrylamide (*meta*-PHEO-CHA):  $^1\text{H}$  NMR (300 MHz, DMSO)  $\delta$  10.71 (s, 1H), 9.04 (s, 1H), 7.44 (d,  $J = 15.8$  Hz, 1H), 7.38–7.27 (m, 5H), 7.26–7.19 (m, 1H), 7.13 (d,  $J = 6.3$  Hz, 2H), 6.95 (d,  $J = 8.3$  Hz, 1H), 6.48 (d,  $J = 15.8$  Hz, 1H), 4.22 (t,  $J = 6.8$  Hz, 2H), 3.05 (t,  $J = 6.8$  Hz, 2H).  $^{13}\text{C}$  NMR (75 MHz,

DMSO- $d_6$ )  $\delta$  163.20, 159.25, 138.73, 136.78, 130.45, 129.43, 128.78, 126.76, 120.41, 119.94, 116.31, 113.54, 68.67, 35.41. ESI-HRMS ( $m/z$ ): Calcd for  $\text{C}_{17}\text{H}_{17}\text{NO}_3$   $[\text{M}+\text{H}]^+$  284.1281, found 284.1280; calcd  $[\text{M}+\text{K}]^+$  322.0840, found 322.0843.

(*E*)-*N*-Hydroxy-3-(4-phenethoxyphenyl)acrylamide (*para*-PHEO-CHA):  $^1\text{H}$  NMR (400 MHz, DMSO)  $\delta$  10.64 (bs, 1H), 8.96 (bs, 1H), 7.48 (d,  $J = 8.3$  Hz, 2H), 7.40 (d,  $J = 15.8$  Hz, 1H), 7.35–7.27 (m, 4H), 7.25–7.19 (m, 1H), 6.96 (d,  $J = 8.6$  Hz, 2H), 6.32 (d,  $J = 15.8$  Hz, 1H), 4.22 (t,  $J = 6.8$  Hz, 2H), 3.03 (t,  $J = 6.8$  Hz, 2H).  $^{13}\text{C}$  NMR (101 MHz, DMSO- $d_6$ )  $\delta$  163.14, 159.43, 138.19, 137.97, 128.99, 128.89, 128.25, 127.40, 126.24, 116.52, 114.85, 68.20, 34.79. ESI-HRMS ( $m/z$ ): Calcd for  $\text{C}_{17}\text{H}_{17}\text{NO}_3$   $[\text{M}+\text{H}]^+$  284.1281, found 284.1292; calcd  $[\text{M}+\text{Na}]^+$  306.1101, found 306.1115.

(ii) Preparation of *ortho*-, *meta*- and *para*-PHEO-CA was performed exactly as described for PhO-CA in section 4.1.3, except that after cooling and stirring for 30 min the obtained conglomeration of oily crystals was carefully crushed up and the resulting solids were filtered, washed 3 times with  $\text{H}_2\text{O}$  (30 ml) and air dried. The yields of the corresponding structural isomers were 98, 84 and 88%.

(*E*)-3-(2-Phenethoxyphenyl)acrylic acid (*ortho*-PHEO-CA):  $^1\text{H}$  NMR (400 MHz, DMSO)  $\delta$  12.26 (bs, 1H), 7.84 (d,  $J = 16.2$  Hz, 1H), 7.64 (d,  $J = 7.6$  Hz, 1H), 7.41–7.26 (m, 5H), 7.21 (t,  $J = 7.1$  Hz, 1H), 7.07 (d,  $J = 8.2$  Hz, 1H), 6.96 (t,  $J = 7.4$  Hz, 1H), 6.50 (d,  $J = 16.2$  Hz, 1H), 4.25 (t,  $J = 6.6$  Hz, 2H), 3.08 (t,  $J = 6.6$  Hz, 2H).  $^{13}\text{C}$  NMR (101 MHz, DMSO)  $\delta$  167.79, 156.87, 138.76, 138.25, 131.61, 129.00, 128.48, 128.24, 126.24, 122.58, 120.67, 119.31, 112.47, 68.77, 34.95. ESI-HRMS ( $m/z$ ): Calcd for  $\text{C}_{17}\text{H}_{16}\text{O}_3$   $[\text{M}+\text{H}]^+$  269.1172, found 269.1175; calcd  $[\text{M} + \text{NH}_4]^+$  286.1438, found 286.1441; calcd  $[\text{M}+\text{Na}]^+$  291.0992, found 291.0995; calcd  $[2\text{M} + \text{Na}]^+$  559.2091, found 559.2102.

(*E*)-3-(3-Phenethoxyphenyl)acrylic acid (*meta*-PHEO-CA):  $^1\text{H}$  NMR (400 MHz, DMSO)  $\delta$  12.39 (s, 1H), 7.55 (d,  $J = 16.0$  Hz, 1H), 7.39–7.17 (m, 9H), 6.97 (dd,  $J = 8.0, 1.7$  Hz, 1H), 6.55 (d,  $J = 16.0$  Hz, 1H), 4.23 (t,  $J = 6.9$  Hz, 2H), 3.04 (t,  $J = 6.9$  Hz, 2H).  $^{13}\text{C}$  NMR (101 MHz, DMSO)  $\delta$  167.57, 158.78, 143.86, 138.30, 135.70, 129.91, 128.96, 128.30, 126.27, 120.82, 119.57, 116.80, 113.42, 68.21, 34.93. ESI-HRMS ( $m/z$ ): Calcd for  $\text{C}_{17}\text{H}_{16}\text{O}_3$   $[\text{M}+\text{H}]^+$  269.1172, found 269.1178; calcd  $[\text{M} + \text{NH}_4]^+$  286.1438, found 286.1447; calcd  $[\text{M}+\text{Na}]^+$  291.0992, found 291.0995; calcd  $[2\text{M} + \text{Na}]^+$  559.2091, found 559.2108; calcd  $[6\text{M} + \text{K}]^{2+}$  824.3151, found 824.3120; calcd  $[7\text{M} + \text{K}]^{2+}$  958.3700, found 958.3665; calcd  $[8\text{M} + \text{K}]^{2+}$  1092.4250, found 1092.4213.

(*E*)-3-(4-Phenethoxyphenyl)acrylic acid (*para*-PHEO-CA):  $^1\text{H}$  NMR (400 MHz, DMSO)  $\delta$  12.19 (s, 1H), 7.60 (d,  $J = 8.6$  Hz, 2H), 7.54 (d,  $J = 16.0$  Hz, 1H), 7.39–7.26 (m, 4H), 7.22 (dt,  $J = 8.1, 4.1$  Hz, 1H), 6.96 (d,  $J = 8.6$  Hz, 2H), 6.36 (d,  $J = 16.0$  Hz, 1H), 4.23 (t,  $J = 6.8$  Hz, 2H), 3.03 (t,  $J = 6.8$  Hz, 2H).  $^{13}\text{C}$  NMR (101 MHz, DMSO)  $\delta$  167.75, 160.07, 143.64, 138.15, 129.87, 128.89, 128.26, 126.82, 126.25, 116.49, 114.83, 68.23, 34.78. ESI-HRMS ( $m/z$ ): Calcd for  $\text{C}_{17}\text{H}_{16}\text{O}_3$   $[\text{M}+\text{H}]^+$  269.1172, found 269.1175; calcd  $[\text{M}+\text{Na}]^+$  291.0992, found 291.1000; calcd  $[2\text{M} + \text{Na}]^+$  559.2091, found 559.2105; calcd  $[6\text{M} + \text{K}]^{2+}$  824.3151, found 824.3110; calcd  $[7\text{M} + \text{K}]^{2+}$  958.3700, found 958.3663; calcd  $[4\text{M} + \text{Na}]^+$  1111.4029, found 1111.3984; calcd  $[5\text{M} + \text{Na}]^+$  1379.5129, found 1379.5067.

(i) Preparation of *ortho*-PHEO-BA. Phenethyl bromide (3.70 g, 20 mmol),  $\text{K}_2\text{CO}_3$  (3.04 g, 22 mmol) and TEBAC (0.50 g, 2.2 mmol) were added to the solution of salicylic aldehyde (2.68 g, 22 mmol) in DMF (20 mL). The reaction mixture was stirred at 90°C for 1 h, followed by supplementing of the additional portion of phenethyl bromide (1.85 g, 10 mmol) and  $\text{K}_2\text{CO}_3$  (3.04 g, 22 mmol) into the vessel, after which heating and stirring continued for 1 h 40 min. After cooling, the vessel contents were filtered, salts were washed 2 times on a filter with *o*-xylol (10 ml) and combined filtrates were evaporated. The residue was dissolved in DCM (50 ml) and washed 2 times with 1 M KOH (40 ml), followed by  $\text{H}_2\text{O}$  (40 ml, 2 times) and

brine (40 ml); the organic layer was dried over  $\text{Na}_2\text{SO}_4$  and evaporated. A spontaneous crystallization of the product took place within 10 min, after which the crude product was resuspended in hexane (20 ml), filtered and air dried. The yield was 47%.

**2-Phenethoxybenzaldehyde (ortho-PHEO-BA):**  $^1\text{H}$  NMR (400 MHz, DMSO)  $\delta$  10.29 (s, 1H), 7.74–7.54 (m, 2H), 7.44–7.27 (m, 4H), 7.27–7.17 (m, 2H), 7.04 (t,  $J = 7.5$  Hz, 1H), 4.34 (t,  $J = 6.6$  Hz, 2H), 3.10 (t,  $J = 6.5$  Hz, 2H).  $^{13}\text{C}$  NMR (101 MHz, DMSO)  $\delta$  189.02, 160.81, 138.23, 136.36, 128.96, 128.26, 127.43, 126.29, 124.24, 120.64, 113.58, 69.01, 34.78. ESI-HRMS ( $m/z$ ): Calcd for  $\text{C}_{15}\text{H}_{14}\text{O}_2$   $[\text{M}+\text{H}]^+$  227.1067, found 227.1068; calcd  $[\text{M}+\text{Na}]^+$  249.0886, found 249.0893.

(i) Preparation of *meta*- and *para*-PHEO-BA. Phenethyl bromide (1.85 g, 10 mmol),  $\text{K}_2\text{CO}_3$  (1.52 g, 11 mmol) were added to the solution of the corresponding aldehyde (1.22 g, 10 mmol) in DMF (10 mL). The reaction mixture was stirred at  $90^\circ\text{C}$  for 2 h. After cooling, the vessel contents were filtered, salts were washed on a filter with *o*-xylol ( $2 \times 5$  ml) and combined filtrates were evaporated. The residue was dissolved in DCM (25 ml) and washed 2 times with 1 M KOH (40 ml), followed by  $\text{H}_2\text{O}$  (40 ml, 2 times) and brine (40 ml); the organic layer was dried over  $\text{Na}_2\text{SO}_4$  and evaporated. The product was isolated by silica gel chromatography using a *n*-hexane–EtOAc mixture (6 : 1) as an eluent. The yields of *m*- and *p*-PHEO-BA in the form of oily liquid were 33 and 31%, respectively.

**3-Phenethoxybenzaldehyde (meta-PHEO-BA):**  $^1\text{H}$  NMR (400 MHz, DMSO- $d_6$ )  $\delta$  9.96 (s, 1H), 7.53–7.47 (m, 2H), 7.45–7.41 (m, 1H), 7.36–7.20 (m, 6H), 4.27 (t,  $J = 6.8$  Hz, 2H), 3.06 (t,  $J = 6.8$  Hz, 2H).  $^{13}\text{C}$  NMR (101 MHz, DMSO)  $\delta$  192.92, 158.91, 138.18, 137.63, 130.35, 128.93, 128.29, 126.29, 122.16, 121.27, 113.95, 68.41, 34.78. ESI-HRMS ( $m/z$ ): not determined.

**4-Phenethoxybenzaldehyde (para-PHEO-BA):**  $^1\text{H}$  NMR (400 MHz, DMSO)  $\delta$  9.86 (s, 1H), 7.85 (d,  $J = 8.8$  Hz, 2H), 7.38–7.27 (m, 4H), 7.26–7.19 (m, 1H), 7.12 (d,  $J = 8.7$  Hz, 2H), 4.30 (t,  $J = 6.9$  Hz, 2H), 3.06 (t,  $J = 6.8$  Hz, 2H).  $^{13}\text{C}$  NMR (101 MHz, DMSO)  $\delta$  191.24, 163.40, 138.01, 131.80, 129.64, 128.96, 128.33, 126.36, 114.95, 68.61, 34.71. ESI-HRMS ( $m/z$ ): not determined.

#### 4.1.6. Synthesis of *ortho*-, *meta*- and *para*-PEGO-CHA

(iii) To a solution of the corresponding acid (0.85 g, 3.0 mmol) in DMF (3 ml), CDI (0.50 g, 3.0 mmol) was added. After 2 h incubation,  $\text{NH}_2\text{OH} \cdot \text{HCl}$  (0.21 g, 3.0 mmol) was added, the mixture was stirred for 15 min and kept overnight (~18 h). The solution was poured into  $\text{H}_2\text{O}$  (9 ml), and after 1 h the precipitate was filtered and air dried. The product was purified by recrystallization. Recrystallizing solvents were EtOH for *o*- and *p*-PEGO-CHA and EtOAc for *m*-PEGO-CHA. The yields of *o*-, *m*- and *p*-PEGO-CHA were 17, 35 and 17%, respectively.

**(E)-N-Hydroxy-3-(2-(2-phenoxyethoxy)phenyl)acrylamide (ortho-PEGO-CHA):**  $^1\text{H}$  NMR (300 MHz, DMSO)  $\delta$  10.02 (bs, 2H), 7.75 (d,  $J = 15.9$  Hz, 1H), 7.54 (d,  $J = 7.3$  Hz, 1H), 7.44–7.26 (m, 3H), 7.15 (d,  $J = 8.1$  Hz, 1H), 7.09–6.92 (m, 4H), 6.53 (d,  $J = 16.0$  Hz, 1H), 4.40 (s, 4H).  $^{13}\text{C}$  NMR (75 MHz, DMSO)  $\delta$  163.56, 158.79, 157.03, 133.62, 131.25, 130.00, 128.19, 124.16, 121.58, 121.28, 120.06, 115.15, 113.53, 67.57, 66.65. ESI-HRMS ( $m/z$ ): Calcd for  $\text{C}_{17}\text{H}_{17}\text{NO}_4$   $[\text{M}+\text{H}]^+$  300.1230, found 300.1231; calcd  $[\text{M}+\text{Na}]^+$  322.1050, found 322.1049.

**(E)-N-Hydroxy-3-(3-(2-phenoxyethoxy)phenyl)acrylamide (meta-PEGO-CHA):**  $^1\text{H}$  NMR (400 MHz, DMSO- $d_6$ )  $\delta$  10.57 (bs, 1H), 9.21 (bs, 1H), 7.44 (d,  $J = 15.7$  Hz, 1H), 7.37–7.24 (m, 3H), 7.16 (d,  $J = 8.3$  Hz, 2H), 7.06–6.86 (m, 4H), 6.48 (d,  $J = 15.8$  Hz, 1H), 4.62–4.13 (m, 4H).  $^{13}\text{C}$  NMR (101 MHz, DMSO- $d_6$ )  $\delta$  162.62, 158.67, 158.27, 138.15, 136.35, 130.00, 129.51, 120.75, 119.93, 119.53, 115.75, 114.48, 113.39, 66.38, 66.15. ESI-HRMS ( $m/z$ ): Calcd for  $\text{C}_{17}\text{H}_{17}\text{NO}_4$   $[\text{M}+\text{H}]^+$  300.1230, found 300.1234; calcd  $[\text{M}+\text{Na}]^+$  322.1050, found

322.1051.

**(E)-N-Hydroxy-3-(4-(2-phenoxyethoxy)phenyl)acrylamide (para-PEGO-CHA):**  $^1\text{H}$  NMR (400 MHz, DMSO- $d_6$ )  $\delta$  9.96 (bs, 2H), 7.51 (d,  $J = 8.2$  Hz, 2H), 7.42 (d,  $J = 15.8$  Hz, 1H), 7.30 (t,  $J = 7.9$  Hz, 2H), 7.04–6.92 (m, 5H), 6.33 (d,  $J = 15.8$  Hz, 1H), 4.33 (dd,  $J = 13.3, 5.0$  Hz, 4H).  $^{13}\text{C}$  NMR (101 MHz, DMSO- $d_6$ )  $\delta$  163.06, 159.34, 158.25, 137.88, 129.49, 129.03, 127.64, 120.74, 116.70, 114.91, 114.47, 66.49, 66.11. ESI-HRMS ( $m/z$ ): Calcd for  $\text{C}_{17}\text{H}_{17}\text{NO}_4$   $[\text{M}+\text{H}]^+$  300.1230, found 300.1236; calcd  $[\text{M}+\text{Na}]^+$  322.1050, found 322.1055.

(ii) Preparation of *ortho*-, *meta*- and *para*-PEGO-CA was performed exactly as described for PHEO-CA in section 4.1.5. The yields of the corresponding structural isomers were 97, 94 and 93%.

**(E)-3-(2-(2-Phenoxyethoxy)phenyl)acrylic acid (ortho-PEGO-CA):**  $^1\text{H}$  NMR (400 MHz, DMSO- $d_6$ )  $\delta$  12.29 (s, 1H), 7.87 (d,  $J = 16.2$  Hz, 1H), 7.69 (d,  $J = 7.7$  Hz, 1H), 7.40 (t,  $J = 7.8$  Hz, 1H), 7.30 (t,  $J = 8.0$  Hz, 2H), 7.15 (d,  $J = 8.3$  Hz, 1H), 7.09–6.97 (m, 3H), 6.95 (t,  $J = 7.3$  Hz, 1H), 6.57 (d,  $J = 16.2$  Hz, 1H), 4.52–4.22 (m, 4H).  $^{13}\text{C}$  NMR (101 MHz, DMSO)  $\delta$  167.89, 158.32, 156.88, 138.77, 131.69, 129.53, 128.71, 122.93, 121.13, 120.84, 119.54, 114.67, 113.07, 67.12, 66.19. ESI-HRMS ( $m/z$ ): Calcd for  $\text{C}_{17}\text{H}_{16}\text{O}_4$   $[\text{M}+\text{H}]^+$  285.1121, found 285.1125; calcd  $[\text{M} + \text{NH}_4]^+$  302.1387, found 302.1392; calcd  $[\text{M}+\text{Na}]^+$  307.0941, found 307.0944; calcd  $[2 \text{ M} + \text{NH}_4]^+$  586.2435, found 586.2450; calcd  $[2 \text{ M} + \text{Na}]^+$  591.1989, found 591.2004.

**(E)-3-(3-(2-Phenoxyethoxy)phenyl)acrylic acid (meta-PEGO-CA):**  $^1\text{H}$  NMR (400 MHz, DMSO)  $\delta$  12.36 (bs, 1H), 7.57 (d,  $J = 16.0$  Hz, 1H), 7.37–7.23 (m, 5H), 7.06–6.90 (m, 4H), 6.57 (d,  $J = 16.0$  Hz, 1H), 4.41–4.26 (m, 4H).  $^{13}\text{C}$  NMR (101 MHz, DMSO)  $\delta$  167.51, 158.65, 158.26, 143.75, 135.71, 129.93, 129.48, 120.98, 120.71, 119.63, 116.74, 114.45, 113.47, 66.42, 66.14. ESI-HRMS ( $m/z$ ): Calcd for  $\text{C}_{17}\text{H}_{16}\text{O}_4$   $[\text{M}+\text{H}]^+$  285.1121, found 285.1124; calcd  $[\text{M} + \text{NH}_4]^+$  302.1387, found 302.1392; calcd  $[\text{M}+\text{Na}]^+$  307.0941, found 307.0945; calcd  $[2 \text{ M} + \text{NH}_4]^+$  586.2435, found 586.2451; calcd  $[2 \text{ M} + \text{Na}]^+$  591.1989, found 591.2001; calcd  $[5 \text{ M} + \text{K}]^{2+}$  730.2474, found 730.2431; calcd  $[6 \text{ M} + \text{K}]^{2+}$  872.2998, found 872.2943; calcd  $[7 \text{ M} + \text{K}]^{2+}$  1014.3522, found 1014.346813; calcd  $[8 \text{ M} + \text{K}]^{2+}$  1156.4047, found 1156.4006.

**(E)-3-(4-(2-Phenoxyethoxy)phenyl)acrylic acid (para-PEGO-CA):**  $^1\text{H}$  NMR (400 MHz, DMSO- $d_6$ )  $\delta$  12.19 (s, 1H), 7.64 (d,  $J = 8.7$  Hz, 2H), 7.56 (d,  $J = 16.0$  Hz, 1H), 7.36–7.24 (m, 2H), 7.02 (d,  $J = 8.8$  Hz, 2H), 6.98 (d,  $J = 8.1$  Hz, 2H), 6.94 (d,  $J = 7.3$  Hz, 1H), 6.39 (d,  $J = 16.0$  Hz, 1H), 4.39–4.28 (m, 4H).  $^{13}\text{C}$  NMR (101 MHz, DMSO)  $\delta$  167.74, 159.98, 158.24, 143.60, 129.90, 129.48, 127.04, 120.75, 116.65, 114.87, 114.47, 66.53, 66.08. ESI-HRMS ( $m/z$ ): Calcd for  $\text{C}_{17}\text{H}_{16}\text{O}_4$   $[\text{M}+\text{H}]^+$  285.1121, found 285.1129; calcd  $[\text{M} + \text{NH}_4]^+$  302.1387, found 302.1393; calcd  $[\text{M}+\text{Na}]^+$  307.0941, found 307.0951; calcd  $[2 \text{ M} + \text{Na}]^+$  591.1989, found 591.2008.

(i) Preparation of *ortho*-PEGO-BA. 2-phenoxyethyl bromide (4.02 g, 20 mmol),  $\text{K}_2\text{CO}_3$  (3.04 g, 22 mmol) and TEBAAC (0.50 g, 2.2 mmol) were added to the solution of salicylic aldehyde (2.68 g, 22 mmol) in DMF (20 mL). The reaction mixture was stirred at  $90^\circ\text{C}$  for 45 min. After cooling to room temperature, the vessel contents were filtered, salts were washed on a filter with *o*-xylol ( $2 \times 10$  ml) and combined filtrates were evaporated. The residue was suspended in MeOH (10 ml); after incubation at  $10^\circ\text{C}$  for 45 min, the precipitate was filtered, washed 2 times on a filter with MeOH (10 ml) and air dried. The yield of *o*-PEGO-BA was 48%.

**2-(2-Phenoxyethoxy)benzaldehyde (ortho-PEGO-BA):**  $^1\text{H}$  NMR (400 MHz, DMSO)  $\delta$  10.34 (s, 1H), 7.74–7.61 (m, 2H), 7.37–7.23 (m, 3H), 7.09 (t,  $J = 7.5$  Hz, 1H), 7.03–6.90 (m, 3H), 4.48 (dd,  $J = 5.4, 3.3$  Hz, 2H), 4.39 (dd,  $J = 5.5, 3.2$  Hz, 2H).  $^{13}\text{C}$  NMR (101 MHz, DMSO- $d_6$ )  $\delta$  189.15, 160.84, 158.36, 136.40, 129.52, 127.51, 124.51, 121.05, 120.85, 114.63, 114.04, 67.63, 66.11. ESI-HRMS ( $m/z$ ): Calcd

for  $C_{15}H_{14}O_3$   $[M+H]^+$  243.1016, found 243.1019; calcd  $[M+Na]^+$  265.0835, found 265.0841.

(i) Preparation of *meta*- and *para*-PEGO-BA. 2-Phenoxyethyl bromide (4.02 g, 20 mmol) and  $K_2CO_3$  (2.76 g, 20 mmol) were added to the solution of the corresponding hydroxybenzaldehyde (2.44 g, 20 mmol) in DMF (20 mL). The reaction mixture was stirred during its heating from 70 °C to 90 °C within 1.5 h and incubated at 90 °C for another 30 min. After cooling to room temperature, the vessel contents were poured into  $H_2O$  (60 ml) and the suspension was stirred at 10 °C for 45 min; the precipitate was filtered, air dried and washed 2 times on a filter with *n*-hexane (5 ml) and air dried. The yields of *m*- and *p*-PEGO-BA were 79 and 76%, respectively.

3-(2-Phenoxyethoxy)benzaldehyde (*meta*-PEGO-BA):  $^1H$  NMR (400 MHz,  $DMSO-d_6$ )  $\delta$  9.99 (s, 1H), 7.59–7.46 (m, 3H), 7.38–7.25 (m, 3H), 7.02–6.89 (m, 3H), 4.40 (dt,  $J = 5.2, 3.1$  Hz, 2H), 4.34 (dt,  $J = 4.5, 3.2$  Hz, 2H).  $^{13}C$  NMR (101 MHz,  $DMSO$ )  $\delta$  192.84, 158.85, 158.23, 137.64, 130.37, 129.49, 122.50, 121.41, 120.75, 114.47, 113.82, 66.69, 66.08. ESI-HRMS ( $m/z$ ): not determined.

4-(2-Phenoxyethoxy)benzaldehyde (*para*-PEGO-BA):  $^1H$  NMR (400 MHz,  $DMSO-d_6$ )  $\delta$  9.88 (s, 1H), 7.88 (d,  $J = 8.6$  Hz, 2H), 7.30 (t,  $J = 7.9$  Hz, 2H), 7.18 (d,  $J = 8.7$  Hz, 2H), 7.01–6.91 (m, 3H), 4.44 (dd,  $J = 5.5, 3.2$  Hz, 2H), 4.34 (dd,  $J = 5.4, 3.2$  Hz, 2H).  $^{13}C$  NMR (101 MHz,  $DMSO-d_6$ )  $\delta$  191.17, 163.23, 158.16, 131.72, 129.76, 129.45, 120.75, 114.94, 114.44, 66.84, 65.94. ESI-HRMS ( $m/z$ ): Calcd for  $C_{15}H_{14}O_3$   $[M+H]^+$  243.1016, found 243.1020.

## 4.2. Biological materials and methods

### 4.2.1. Antiviral activity

The Huh7-luc/neo cell culture was reseeded into a 48-well plate in the medium without antibiotic G418. After 48 h (30–40% monolayer), the studied compounds at different concentrations were added to the culture medium. After the incubation at 37 °C in 5%  $CO_2$  for three days (monolayer in the control probe was 100%), the medium was removed. The cells were washed with phosphate buffered saline (PBS) and lysed, followed by the evaluation of the luciferase activity by the Luciferase Assay System kit (Promega, USA) according to the manufacturer's protocol. Chemiluminescence was measured on a Thermo luminometer (Labsystems, USA).

### 4.2.2. Cell viability

The Huh7 cell culture was reseeded into a 96-well plate. After 24 h (30–40% monolayer), the studied compounds at different concentrations were added to the culture medium. After the incubation at 37 °C in 5%  $CO_2$  for three days (monolayer in the control probe was 100%), the cell viability was evaluated using the MTT kit (Sigma-Aldrich, USA) according to the manufacturer's protocol.

### 4.2.3. Sample preparation for western blot analysis

The cell cultures were reseeded into a 6-well plate. After 24 h (40–50% monolayer), the studied compounds at different concentrations were added to the culture medium. After the incubation at 37 °C in 5%  $CO_2$  for 24 h (monolayer in the control probe was 80–90%), the medium was removed. The cells were washed with PBS, treated with a lysing reagent (Promega, USA), and used in the experiments with  $\alpha$ -tubulin and SMC3. To extract H3 histone, the cells were separated from the plate by a scraper and centrifuged (13,400 rpm, 1 min), followed by the addition of a lysing TEB buffer containing 1xPBS, 0.5% Triton-X100 (v/v), and 2 mM phenylmethylsulfonyl fluoride (400  $\mu$ L). The cells were lysed for 10 min at 4 °C, followed by centrifugation (8400 rpm, 10 min) at 4 °C. The supernatant was removed; the residue was washed with TEB (200  $\mu$ L) and centrifuged (8400 rpm, 10 min) at 4 °C. The supernatant was removed, and the pellet was resuspended in 0.2 M HCl (100  $\mu$ L) and left overnight at 4 °C. After centrifugation (8400 rpm,

10 min) at 4 °C, the supernatant was neutralized with 1.5 M Tris-HCl, pH 8.8 (one-tenth of the volume), followed by the addition of a 5x Laemmly buffer (one-fifth of the volume).

### 4.2.4. Western blot

The proteins from the cellular lysates were separated by electrophoresis in 10% PAAG containing 0.1% SDS and then transferred to a nitrocellulose membrane by electroblotting. The membrane was treated with 5% low-fat dry milk (Bio-Rad, USA) in PBS that contained 0.05% Tween-20 (PBST) for 60 min at room temperature. The primary antibodies in dilution 1 : 10,000 were added to  $\alpha$ -tubulin (T5168, Sigma, USA); in dilution 1 : 2000 to histone H3 (9715S, CST) and SMC3 (5996S, CST); in dilution 1 : 1000 to the acetylated form of  $\alpha$ -tubulin (anti-acetyl lysine antibody, ab80178, Abcam, UK) and the acetylated form of histone H3 (anti-acetyl histone H3(K9/K14), 9677S, CST); in dilution 1 : 500 to the acetylated form of SMC3K105/106ac (anti-acetyl SMC3 antibody (K105/106), MABE1073, EMD Millipore, USA). The mixtures were incubated overnight at 4 °C, followed by washing with PBST. The conjugate of horseradish peroxidase with secondary specific antibodies (anti-mouse and anti-rabbit, Santa Cruz, USA) were added in dilution 1 : 10,000, and the mixtures were incubated for 50 min at room temperature. The membranes were washed with PBST, and the signal was visualized using the ECL kit (Pierce-Thermo Scientific, USA) and High-performance ECL film (GE Healthcare, USA).

### 4.2.5. Statistical analysis

Data on the luciferase activity and cell viability were presented as the mean value and standard deviation of at least four and six independent experiments, correspondingly. The extent of correlation between two variables was quantified by calculating the Pearson's product moment correlation coefficient ( $r$ ), while its significance ( $P$ ) was evaluated by the  $t$ -test.

## Acknowledgments

The work was supported by the Russian Foundation for Basic Research (Grant # 17-04-00175) and by the Program of Fundamental Research of the State Academies of Sciences (Grant # 01201363818).

## References

- [1] R. Bartenschlager, T.F. Baumert, J. Bukh, M. Houghton, S.M. Lemon, B.D. Lindenbach, V. Lohmann, D. Moradpour, T. Pietschmann, C.M. Rice, R. Thimme, T. Wakita, Critical challenges and emerging opportunities in hepatitis C virus research in an era of potent antiviral therapy: considerations for scientists and funding agencies, *Virus Res.* 248 (2018) 53–62, <https://doi.org/10.1016/j.virusres.2018.02.016>.
- [2] M.B. Zeisel, E. Crouchet, T.F. Baumert, C. Schuster, Host-targeting agents to prevent and cure hepatitis C virus infection, *Viruses* 7 (2015) 5659–5685, <https://doi.org/10.3390/v7112898>.
- [3] N. Hamdane, F. Jühling, E. Crouchet, H.E. Saghire, C. Thumann, M.A. Oudot, S. Bandiera, A. Saviano, C. Ponsolles, A.A. Suarez, S. Li, N. Fujiwara, A. Ono, I. Davidson, N. Bardeesy, C. Schmidl, C. Bock, C. Schuster, J. Lupberger, F. Habersetzer, M. Doffoel, T. Piardi, D. Sommacale, M. Imamura, T. Uchida, H. Ohdan, H. Aikata, K. Chayama, T. Boldanova, P. Pessaux, B.C. Fuchs, Y. Hoshida, M.B. Zeisel, F.H. Duong, T.F. Baumert, HCV-induced epigenetic changes associated with liver cancer risk persist after sustained virologic response, *Gastroenterology* 156 (2019) 2313–2329, <https://doi.org/10.1053/j.gastro.2019.02.038>.
- [4] J. Chen, N. Wang, M. Dong, M. Guo, Y. Zhao, Z. Zhuo, C. Zhang, X. Chi, Y. Pan, J. Jiang, H. Tang, J. Niu, D. Yang, Z. Li, X. Han, Q. Wang, X. Chen, The metabolic regulator histone deacetylase 9 contributes to glucose homeostasis abnormality induced by hepatitis C virus infection, *Diabetes* 64 (2015) 4088–4098, <https://doi.org/10.2337/db15-0197>.
- [5] J. Chen, Z. Zhang, N. Wang, M. Guo, X. Chi, Y. Pan, J. Jiang, J. Niu, S. Ksimu, J.Z. Li, X. Chen, Q. Wang, Role of HDAC9-FoxO1 axis in the transcriptional program associated with hepatic gluconeogenesis, *Sci. Rep.* 7 (1) (2017) 6102, <https://doi.org/10.1038/s41598-017-06328-3>.
- [6] E. Seto, M. Yoshida, Erasers of histone acetylation: the histone deacetylase

- enzymes, *Cold Spring Harb. Perspect. Biol.* 6 (2014), a018713, <https://doi.org/10.1101/cshperspect.a018713>.
- [7] M. Martin, R. Kettmann, F. Dequiedt, Class IIa histone deacetylases: regulating the regulators, *Oncogene* 26 (2007) 5450–5467, <https://doi.org/10.1038/sj.onc.1210613>.
- [8] X.J. Yang, E. Seto, The Rpd3/Hda1 family of lysine deacetylases: from bacteria and yeast to mice and men, *Nat. Rev. Mol. Cell Biol.* 9 (2008) 206–218, <https://doi.org/10.1038/nrm2346>.
- [9] K. Miura, K. Taura, Y. Kodama, B. Schnabl, D.A. Brenner, Hepatitis C virus-induced oxidative stress suppresses hepcidin expression through increased histone deacetylase activity, *Hepatology* 48 (2008) 1420–1429, <https://doi.org/10.1002/hep.22486>.
- [10] H. Liu, T.L. Trinh, H. Dong, R. Keith, D. Nelson, C. Liu, Iron regulator hepcidin exhibits antiviral activity against hepatitis C virus, *PLoS One* 7 (10) (2012), e46631, <https://doi.org/10.1371/journal.pone.0046631>.
- [11] A. Sato, Y. Saito, K. Sugiyama, N. Sakasegawa, T. Muramatsu, S. Fukuda, M. Yoneya, M. Kimura, H. Ebinuma, T. Hibi, M. Ikeda, N. Kato, H. Saito, Suppressive effect of the histone deacetylase inhibitor suberoylanilide hydroxamic acid (SAHA) on hepatitis C virus replication, *J. Cell. Biochem.* 114 (2013) 1987–1996, <https://doi.org/10.1002/jcb.24541>.
- [12] Y. Zhou, Q. Wang, Q. Yang, J. Tang, C. Xu, D. Gai, X. Chen, J. Chen, Histone deacetylase 3 inhibitor suppresses hepatitis C virus replication by regulating Apo-A1 and LEAP-1 expression, *Virology* 533 (2018) 418–428, <https://doi.org/10.1007/s12250-018-0057-7>.
- [13] Y. Liu, L. Peng, E. Seto, S. Huang, Y. Qiu, Modulation of histone deacetylase 6 (HDAC6) nuclear import and tubulin deacetylase activity through acetylation, *J. Biol. Chem.* 287 (2012) 29168–29174, <https://doi.org/10.1074/jbc.M112.371120>.
- [14] M.V. Kozlov, A.A. Kleymenova, K.A. Konduktorov, A.Z. Malikova, S.N. Kochetkov, Selective inhibitor of histone deacetylase 6 (tubastatin A) suppresses proliferation of hepatitis C virus replicon in culture of human hepatocytes, *Biochemistry (Mosc.)* 79 (2014) 637–642, <https://doi.org/10.1134/S0006297914070050>.
- [15] C. Seidel, M. Schneckeburger, M. Dicato, M. Diederich, Histone deacetylase 6 in health and disease, *Epigenomics* 7 (2015) 103–118, <https://doi.org/10.2217/EPI.14.69>.
- [16] L. Zhang, A. Ogden, R. Aneja, J. Zhou, Diverse roles of HDAC6 in viral infection: implications for antiviral therapy, *Pharmacol. Ther.* 164 (2016) 120–125, <https://doi.org/10.1016/j.pharmthera.2016.04.005>.
- [17] K. Zheng, Y. Jiang, Z. He, K. Kitazato, Y. Wang, Cellular defence or viral assist: the dilemma of HDAC6, *J. Gen. Virol.* 98 (2017) 322–337, <https://doi.org/10.1099/jgv.0.000679>.
- [18] J. Roche, P. Bertrand, Inside HDACs with more selective HDAC inhibitors, *Eur. J. Med. Chem.* 121 (2016) 451–483, <https://doi.org/10.1016/j.ejmech.2016.05.047>.
- [19] W.J. Huang, Y.C. Wang, S.W. Chao, C.Y. Yang, L.C. Chen, M.H. Lin, W.C. Hou, M.Y. Chen, T.L. Lee, P. Yang, C.I. Chang, Synthesis and biological evaluation of ortho-aryl N-hydroxycinnamides as potent histone deacetylase (HDAC) 8 isoform-selective inhibitors, *ChemMedChem* 7 (2012) 1815–1824, <https://doi.org/10.1002/cmdc.201200300>.
- [20] T. Ai, Y. Xu, L. Qiu, R.J. Geraghty, L. Chen, Hydroxamic acids block replication of hepatitis C virus, *J. Med. Chem.* 58 (2015) 785–800, <https://doi.org/10.1021/jm501330g>.
- [21] M.V. Kozlov, A.A. Kleymenova, K.A. Konduktorov, A.Z. Malikova, K.A. Kamarova, R.A. Novikov, S.N. Kochetkov, Synthesis of (Z)-N-hydroxy-3-methoxy-3-phenylacrylamide as new selective inhibitor of hepatitis C virus replication, *Russ. J. Bioorganic Chem.* 42 (2016) 191–197, <https://doi.org/10.1134/S1068162016010076>.
- [22] M.V. Kozlov, A.Z. Malikova, K.A. Kamarova, K.A. Konduktorov, S.N. Kochetkov, Synthesis of pyridyl-4-oxy-substituted N-hydroxy amides of cinnamic acid as new inhibitors of histone deacetylase activity and hepatitis C virus replication, *Russ. J. Bioorganic Chem.* 44 (2018) 453–460, <https://doi.org/10.1134/S1068162018040118>.
- [23] J.M. Vrolijk, A. Kaul, B.E. Hansen, V. Lohmann, B.L. Haagmans, S.W. Schalm, R. Bartenschlager, A replicon-based bioassay for the measurement of interferons in patients with chronic hepatitis C, *J. Virol. Methods* 110 (2003) 201–209, [https://doi.org/10.1016/S0166-0934\(03\)00134-4](https://doi.org/10.1016/S0166-0934(03)00134-4).
- [24] T. Dasgupta, J. Antony, A.W. Braithwaite, J.A. Horsfield, HDAC8 inhibition blocks SMC3 deacetylation and delays cell cycle progression without affecting cohesin-dependent transcription in MCF7 cancer cells, *J. Biol. Chem.* 291 (2016) 12761–12770, <https://doi.org/10.1074/jbc.M115.704627>.
- [25] T. Fujii, Alkali-metal ion/molecule association reactions and their applications to mass spectrometry, *Mass Spectrom. Rev.* 19 (2000) 111–138, [https://doi.org/10.1002/1098-2787\(200005/06\)19:3<111::AID-MA51>3.0.CO;2-K](https://doi.org/10.1002/1098-2787(200005/06)19:3<111::AID-MA51>3.0.CO;2-K).